AUS DEM LEHRSTUHL
FÜR KIEFERORTHOPÄDIE
PROF. DR. DR. P. PROFF
DER FAKULTÄT FÜR MEDIZIN
DER UNIVERSITÄT REGENSBURG

Investigation of Gpx1 in chondrogenesis and its role on redox regulation in chondrocytes

Inaugural – Dissertation
zur Erlangung des Doktorgrades
der Zahnmedizin

der
Fakultät für Medizin
der Universität Regensburg

vorgelegt von
Vasiliki Koretsi

2015

AUS DEM LEHRSTUHL
FÜR KIEFERORTHOPÄDIE
PROF. DR. DR. P. PROFF
DER FAKULTÄT FÜR MEDIZIN
DER UNIVERSITÄT REGENSBURG

Investigation of Gpx1 in chondrogenesis and its role on redox regulation in chondrocytes

Inaugural – Dissertation
zur Erlangung des Doktorgrades
der Zahnmedizin

der
Fakultät für Medizin
der Universität Regensburg

vorgelegt von
Vasiliki Koretsi

2015

Dekan:	Prof. Dr. Dr. Torsten Reichert
1. Berichterstatter:	Prof. Dr. Dr. Peter Proff
2. Berichterstatter:	Prof. Dr. Michael Behr
Tag der mündlichen Prüfung:	05.07.2016

Table of contents

1. Statement of the problem and objectives

The development of cranial base exerts a great influence on the overall facial shape. In the vertical plane, the inclination of the middle cranial fossa affects the position of the nasomaxillary complex in relation to the mandible, thus; influencing the vertical growth of the face. A hypodivergent growth pattern may be due to a forward-downward inclination of the middle cranial fossa, whereas a hyperdivergent growth pattern may be a resultant of posterosuperior inclination of it. Sagittally, Class II skeletal malocclusion is often characterized by one or more of the following: an elongated posterior cranial fossa, a forward and downward position of it, a short composite of ramus and the vertical dimension of posterior cranial fossa, and a more open cranial base flexure. By contrast, Class III skeletal malocclusions often demonstrate a size reduction in the posterior cranial base, a backward alignment of it, a long composite of ramus and the vertical dimension of the posterior cranial fossa, and a relative acute cranial base angle (Enlow and Hans, 1996; Premkumar, 2011).

The process of endochondral ossification characterizes both the development and growth of the cranial base. It is the mechanism by which the cranial base develops from the chondrocranium to the basicranium and also grows at the midline axis postnatally. The midline axis of the cranial base is the region where all the synchondroses are located. It contributes significantly both to elongation and angulation of the cranial base (Sperber, 1989; Proffit et al., 2007). The process of endochondral ossification has been studied extensively. However, it was not until recently that the fundamental role of reactive oxygen species (ROS) was revealed and documented. In particular, hydrogen peroxide (H_2O_2) causes inhibition of proliferating chondrocytes and is required for the normal differentiation of proliferating to hypertrophic chondrocytes (Morita et al., 2007).

The antioxidant enzyme glutathione peroxidase 1 (Gpx1) can efficiently reduce H_2O_2 (Mills, 1957). Provided that no previous research has been undertaken to elucidate the role of Gpx1 on chondrogenic differentiation, the objectives of this study (Koretsi et al., 2015) were:

- Observation and definition of the temporal expression pattern of Gpx1 during chondrogenic differentiation *in vitro*.
- Identification of Gpx1 expression according to the different stages of chondrogenic differentiation.

- Determination of Gpx1 as an antioxidant enzyme capable of regulating redox state in chondrocytes.

2. Review of the literature

2.1. The cranial base

Cranial base is the oldest part of the human skull phylogenetically. It is an integrative component of the skull that serves several functions (Enlow, 1968; Stark, 1975; Knußmann, 1988; Sperber, 2001). It serves as a platform, upon which the brain grows, and provides a thrust for the anterior growth of the facial skeleton. In addition, the cranial base connects the cranium with the rest of the body (articulation with the vertebral column, maxillary region and the mandible, provision of conduits for all the vital neural and circulatory connections, formation of the roof of the nasopharynx) (Premkumar, 2011).

2.1.1. Developmental and anatomical aspects

The human cranial base first appears in the second month of embryonic life as an irregular cartilaginous shape, the chondrocranium. The chondrocranium develops as condensations of the neural crest cells and paraxial mesoderm in the ectomeninx (Sperber, 1989). Nine groups of paired cartilaginous precursors are subsequently formed by the growth and differentiation of the ectomeninx (Kjaer, 1990; Fig. 1).

The cartilaginous precursors anterior to the notochord derive solely from segmented neural crest tissue, similar to other facial bones; while the posterior precursors derive from segmented mesodermal tissue. By this means, the middle of the sphenoid body marks the division between the anterior and posterior portions of the cranial base, which have distinct embryologic origins; the anterior cranial base stemming from the neural crest and the posterior from the paraxial mesoderm (Noden, 1991; Couly et al., 1993; Le Douarin et al., 1993).

Via endochondral ossification from numerous ossification centres, which form a highly perforated irregular mass of cartilages known as basal plate, the chondrocranium is transformed to the basicranium. The proceeding of ossification is initiated from the mesodermally derived cartilages and moves from caudal to rostral and lateral; finally composing the four major bones of the basicranium: the ethmoid, sphenoid, occipital, and temporal bones (Sperber, 1989; Kjaer, 1990; Williams et al., 1995). Sphenoid, occipital, and temporal bones have several contributions from intramembranous bones, whereas ethmoid is exclusively endochondral in origin (Sperber, 2001).

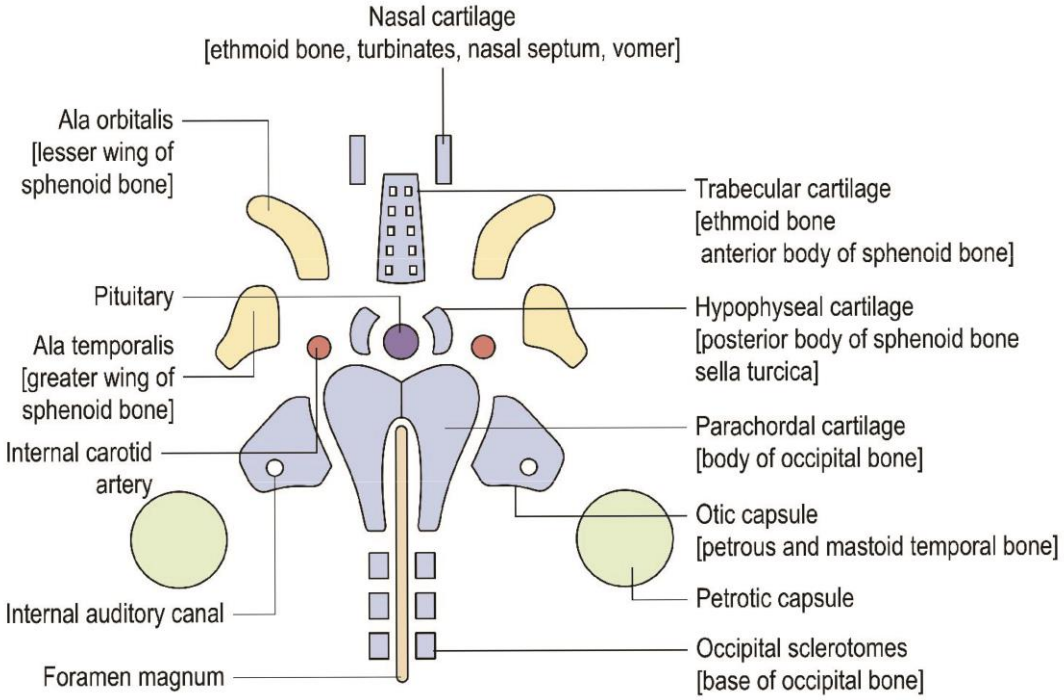

Fig. 1. The cartilages of the chondrocranium (from M. T. Cobourne, A. T. DiBiase, 2010).

Bony elevations divide the cranial base into anterior, middle, and posterior cranial fossae. The lesser wing of the sphenoid marks the division between anterior and middle cranial fossa and the petrous temporal sets the boundaries between middle and posterior cranial fossa. The anterior cranial fossa lies at a superior level compared to middle cranial fossa, which in turn is located more superiorly than the posterior cranial fossa (Premkumar, 2011; Fig. 2).

Basicranial development is governed by three important principles. The centre of the basicranium completes growing faster than the anterior, posterior, and lateral portions; possibly because it is the region where important nerves and vessels penetrate the skull. Furthermore, the anterior and posterior cranial base grow to a certain extent independently; a phenomenon potentially attributed to the distinct embryologic origins of them. Finally, most basicranial growth in the three cranial fossae occurs independently (Sperber, 1989; Lieberman et al., 2000).

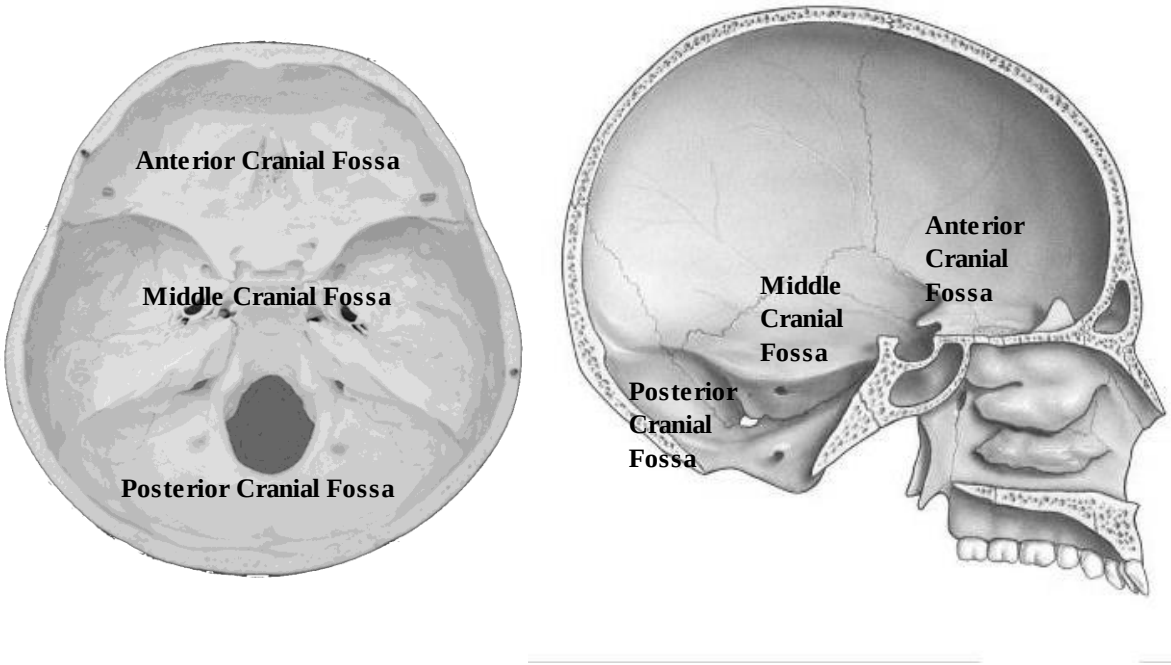

Fig. 2. The cranial fossae, left: superior view, right: lateral view (adapted from F. H. Netter, 2011).

2.1.2. The growth of cranial base and its implications in the facial shape

The growth of cranial base is a complex sequence of events and happens both within and between endocranial fossae. It is accomplished by primary displacement of bone due to expanding lobes of the brain, linear displacement caused by growth at synchondroses and extensive cortical remodelling (Stark, 1975; Premkumar, 2011). Growth occurs as angulation

and in antero-posterior, medio-lateral, and supero-inferior dimensions. The cranial growth plate, which is located at the midline axis of the cranial base and includes the intersphenoidal, spheno-ethmoidal, and spheno-occipital synchondroses, contributes to overall growth of cranial base at the synchondroses via interstitial growth of a pressure-adapted mechanism of endochondral ossification (Enlow and Hans, 1996; Proffit et al., 2007; Fig. 3).

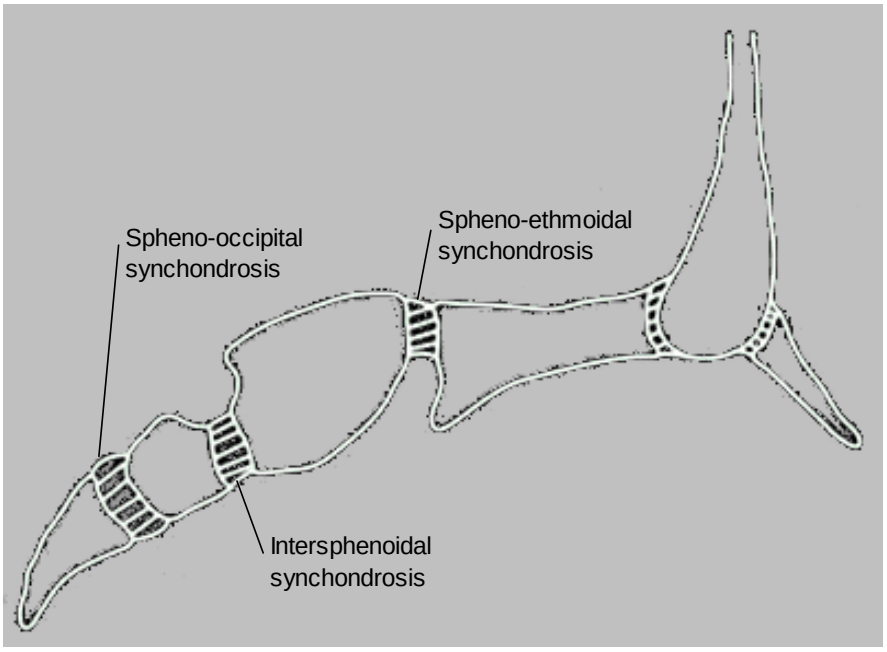

Fig. 3. The synchondroses of the cranial base (adapted from http://www.anthropology.pitt.edu/node/957, last access on 09.01.2016).

Antero-posterior growth is, except for displacement due to growth of functional matrix, attributed to the midline axis of the cranial base where all the synchondroses are located. Postnatally, the posterior cranial base mainly elongates through deposition in the spheno-occipital synchondrosis, whereas anterior cranial base (measured from sella to foramen caecum) through deposition in the spheno-ethmoidal synchondrosis. Anterior cranial base attains approximately 95% of its adult length at approximately six years and spheno-ethmoidal synchondrosis ceases contributing to antero-posterior growth after the age of seven years (Scott, 1958; Stark, 1975; Sperber, 2001).

Medio-lateral growth is not attributed to the cranial growth plate, instead it happens primarily through drift and intramembranous bone growth in sutures with regard to anterior and posterior cranial fossae and through lateral drift of the squamous portions of the sphenoid with regard to the middle cranial fossa. Furthermore, supero-inferior growth occurs through drift, thus also lacking a contribution of the cranial growth plate to growth (Sperber, 1989).

Angulation of cranial base is a unique characteristic of humans and happens as an aftermath of bone or cartilage deposition in the midline axis of the cranial base that changes the angle between intersecting anterior and posterior cranial base. This causes the inferior cranial base angle to become more acute (flexion) or more obtuse (extension) (Lieberman et al., 2000). Cranial base angulation is a resultant of different growth processes at different locations of the cranial base.

All the synchondroses of the cranial base play, among others, a role on angulation of the cranial base via interstitial growth (Bjork, 1955; Scott, 1958; Giles et al., 1981; Enlow, 1990). The prenatal involvement of them in flexion or extension lies on the decreased chondrogenic activity in the inferior vs. superior part of the synchondrosis causing flexion, whereas extension results from a decreased chondrogenic activity in the superior compared to inferior part of the synchondrosis (Hofer, 1960; Hofer and Spatz, 1963; Stark, 1975; Diewert, 1985 Anagastopolou et al., 1988; Sperber, 1989). However, only the spheno-occipital synchondrosis seems to play an important role on cranial base angulation postnatally. It remains an active site until the age of 20 years, while spheno-ethmoidal fuses at six to eight years and intersphenoidal prior to birth (Bjork, 1955; Scott, 1958; Premkumar, 2011).

The fact that cranial base is not flat causes the foramen magnum to have a relatively more anterior position and ventral orientation, which in turn reduces the lever arm between the centre of mass of the head and the atlanto-occipital joint, thereby the magnitude of the force required to hold up the head is reduced (Schultz, 1942). The flexure of human cranial base; it demonstrates an angulation of 65 ° at clivus, between the middle and posterior cranial fossa, contributes to the orthograde posture of man, redirection of the face from forward to downward direction, and anterior and inferior movement of the middle face (Premkumar, 2011).

According to Enlow's (Enlow and Hans, 1996) counterpart principle of craniofacial growth, there are regional relationships throughout the whole face and cranium, which consist of anatomical parts that are directly related to their specific anatomical counterparts. If both parts

and their corresponding counterparts enlarge to the same extent, then balanced growth between them is the result. Imbalances are caused by differences in the amount or direction of growth between parts and their particular counterparts. The upper part of the nasomaxillary complex, the anterior cranial fossa, the palate, and the mandibular corpus are considered by Enlow (Enlow and Hans, 1996) to be the counterparts of bony maxillary arch, while the ramus of the mandible is the structural counterpart of the middle cranial fossa.

Anterior cranial fossa comprises the orbital plates of frontal bone and crista galli. After eight years of age, its lengthening is directly due to growth of functional matrix (Premkumar, 2011). The upper face shares same bony elements with the anterior cranial base resulting in a high degree of integration between these two regions. It seems that anterior cranial base affects the orientation of the upper face directly, but that it only not immediately affects palate orientation through the integration of palate and orbits (Lieberman et al., 2000).

The middle cranial fossa and the ethmomaxillary complex, although they do not demonstrate as tight anatomical relationship as this of anterior cranial base and upper face, interact in a way that the shape of the former seems to influence not only the orientation of the posterior border of the later but also its location in relation to the rest of the cranial base (Hoyte, 1991). Expansion of the middle cranial fossa due to growth of temporal lobe has a secondary displacement effect on anterior cranial fossa, ethmomaxillary complex, and mandible. Because of the position of posterior border of maxillary complex at the intersection between the anterior and middle cranial fossae, the growth of middle cranial fossa displaces forward the anterior cranial fossa and the ethmomaxillary complex suspended beneath it (Enlow and Hans, 1996; Premkumar, 2011). The forward displacement of the mandible is less than this of anterior cranial fossa and ethmomaxillary complex because most of the growth of the middle cranial fossa occurs anterior to mandibular condyles. Additionally, according to Enlow's (Enlow and Hans, 1996) counterpart principle of growth the ramus of the mandible elongates in a matched way to the elongation of the middle cranial fossa resulting in placing the mandibular arch in a more anterior position.

Posterior cranial fossa through the inclination of clivus, where the spheno-occipital synchondrosis is located, is responsible for the anterior and forward growth of the cranial base. Among others, growth of spheno-occipital synchondrosis results in an anterior and inferior displacement through the lengthening of clivus, which orients the nasomaxillary complex downward and forward. In turn, the downward and forward orientation of

nasomaxillary complex affects the vertical dimensions of the middle and lower face (Premkumar, 2011).

2.1.3. Angulation of cranial base and occlusal type

Because of its position, cranial base is difficult to be directly measured. In orthodontics, cranial base is traditionally measured through lateral cephalometric radiographs. A commonly used measurement is the angle nasion-sella-basion. Nasion however is not a satisfactory point because of its position outside the limits of the cranial base and the change in its position with age (Scott, 1958). Alternatively, nasion can be replaced with the foramen caecum or the intersection of the orbital roof and the inner surface of the frontal bone (Lieberman and McCarthy, 1999). Posteriorly, basion is often replaced by articulare and Bolton points (Dhopatkar et al., 2002).

There is an abundance of studies supporting the relationship between cranial base angulation and type of malocclusion. In studies comparing Class II and Class III not only with Class I but also with each other, a progressive increase was found in cranial base angulation from Class III, via Class I, to Class II individuals (Hopkin et al., 1968; Dibbets, 1996). Furthermore, studies comparing Class II with Class I individuals reported a larger cranial base angulation in Class II than Class I individuals (Anderson and Popovich, 1983; Bacon et al., 1992). This feature was found to be related with the prepubertal developmental stage (Kerr and Hirst, 1987; Franchi et al., 2007). As far as Class III malocclusion is concerned, the basicranial angulation was reported more decreased in Class III sample compared with a mixed Class I and II control sample (Proff et al., 2008). Moreover, compared with Class I, Class III malocclusion showed a more prominent cranial base flexure (Mouakeh, 2001; Chang et al., 2005). The alteration in basicranial angulation in Class III malocclusion was related with changes occurring in posterior leg of the cranial base (Chang et al., 2005; Proff et al., 2008), supporting the theory of deficient orthocephalization (Singh et al., 1997).

2.2. The process of endochondral ossification

Endochondral ossification is a mechanism of bone formation defined by the presence of a pre-existing hyaline cartilaginous model of the developing bone. Endochondral ossification is distinguished from intramembranous ossification because of the presence of a hyaline cartilaginous model and the simultaneous presence of cartilage and bone during the ossification process (Henrikson et al., 1997).

2.2.1. Early differentiation of chondrocytes

Chondrogenesis is the process of producing cartilage intermediate that induces endochondral ossification during skeletal development. It includes distinct stages and is initiated by the mesenchymal cell recruitment, migration, proliferation, and condensation. Commitment of mesenchymal cells is strongly dependent on their interactions with the overlying epithelium, which activates signalling pathways and transcription factors (Olsen et al., 2000). Before mesenchymal cells condensate, they produce extracellular matrix containing hyaluronan, collagen type I and IIA (Goldring et al., 2006). Collagen type IIA belongs to non-cartilage collagens, as it is expressed not only by chondroprogenitor cells but somites or epithelial cells as well (Sandell et al., 1994; Fig. 4).

Precartilaginous condensations of chondroprogenitor cells are characterised by increased cell adhesion and formation of gap junctions, and changes in the cytoskeleton (Goldring et al., 2006). An escalation in hyaluronidase activity together with the appearance of cell adhesion molecules, N-cadherin and neural cell adhesion molecule (N-CAM), are evident during this phase. Transforming growth factor (TGF-β), which is an early signal of condensation, triggers the production of fibronectin. The connection of Syndecan to fibronectin reduces N-CAM secretion, thus drawing the boundaries of the condensation (Goldring et al., 2006).

The transition of chondroprogenitors to chondrocytes is commenced by intracellular signalling pathways such as fibroblast growth factors (FGFs), hedgehog , bone morphogenetic proteins (BMPs), and Wnt. Wnt signals are required to induce the production of FGFs, which act in positive feedback loops (Niswander, 2003). The homeodomain (Hox) transcription factors coordinate proliferation of cells within the condensations and they are required for the

FGF-8 and sonic hedgehog (Shh) expression (Goldring et al., 2006). BMPs are vital not only for the formation of precartilaginous condensations but also for the differentiation of chondroprogenitors into chondrocytes (Yoon and Lyons, 2004).

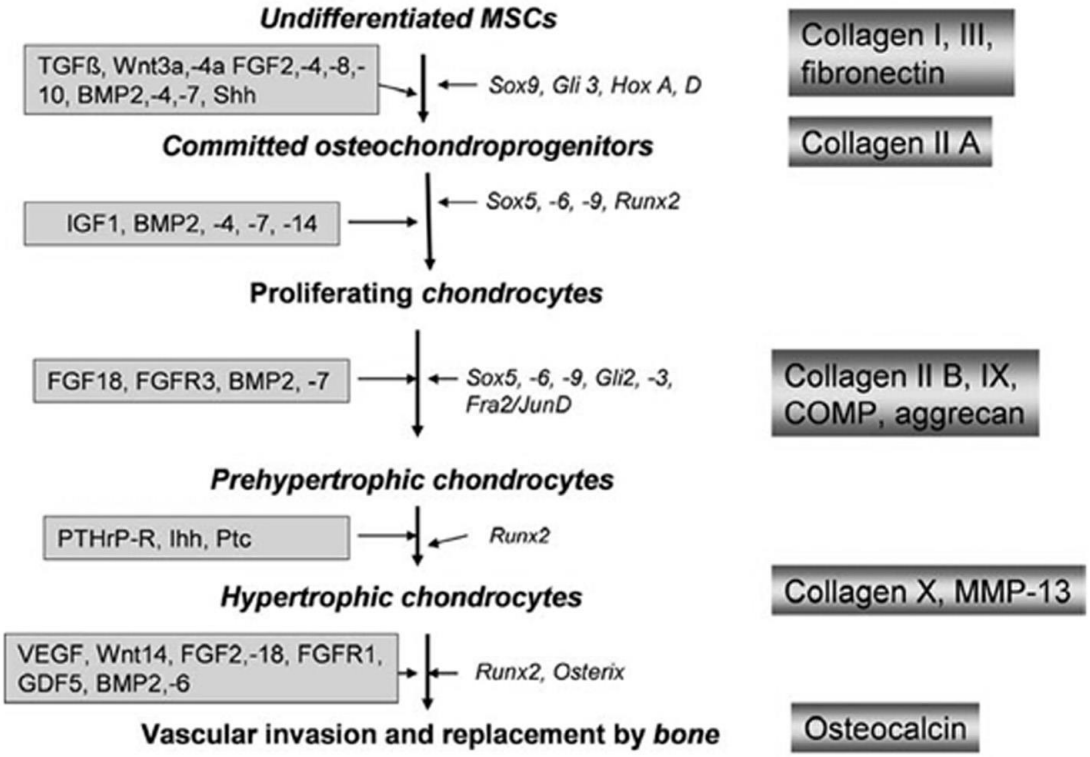

Fig. 4. Early and terminal chondrogenic differentiation. Growth factors and signalling for each differentiation stage are presented on the left and biological markers on the right; MSCs: mesenchymal stem cells (from S. Grassel, N. Ahmed, 2007).

During the differentiation of chondroprogenitors to chondrocytes, BMPs signalling induces the expression of Sox proteins (Yoon et al., 2005). The Sox9 transcription factor is co-expressed with two additional Sox family members and is needed for the collagen II gene to be expressed along with other cartilage-specific matrix proteins (Ng et al., 1997; Lefebvre et al., 2001). BMPs not only induce the expression of various transcription factors but via activation of TGF-β activated kinase 1 (Tak1) can trigger the p38 and JNK cascades (Yoon and Lyons, 2004). The stimulation of chondrogenic cellular condensation is provoked by the

p38 pathway and followed by cartilage nodule formation (Nakamura et al., 1999). During this stage, chondrocytes produce collagens II, IX and XI, and aggrecan.

Subsequently, the differentiated chondrocytes begin to proliferate and form the proliferating zones. Proliferative zones are characterized by the existence of pairs of chondrocytes in a single lacuna within the cartilage matrix (Mackie et al., 2011). Proliferative chondrocytes subsequently separate from each other by an escalation in their secretion activity that features the following late hypertrophic stage (Mackie et al., 2011). The structure of synchondroses is bipolar: a central layer of small cartilaginous cells, with proliferative zone, hypertrophic zone, and zone of endochondral ossification on either side (Premkumar, 2011; Fig. 5).

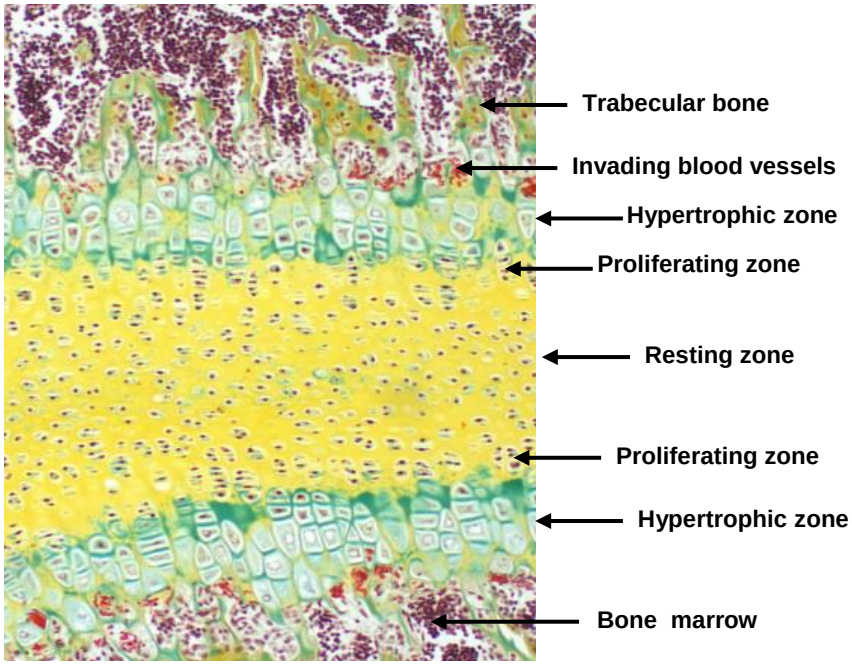

Fig. 5. The bipolar structure of the spheno-occipital synchondrosis of a rat stained with Movat's pentachrome staining, Magn. ×100 (from V. Koretsi et al., 2015).

The systemic regulator growth hormone (GH) stimulates the secretion of insulin-like growth factor 1 (IGF1) and the GH/IGF1 axis plays a key role on promoting chondrocyte proliferation (Nilsson et al., 2005; Pass et al., 2009). Locally, the binding of Wnt family proteins to their receptor can activate either the canonical Wnt signalling pathway or the non-canonical one. The former involves the accumulation of β-catenin, a cytoplasmic protein that

functions in cell to cell adhesion by interacting with cadherins, whereas the latter the degradation of β-catenin. At this stage, Wnt signalling pathways stimulate chondrocyte proliferation (Akiyama et al., 2004; Andrade et al., 2007).

Indian hedgehog (Ihh) is required for normal chondrocyte proliferation throughout the growth plate during both embryonic and postnatal growth and secreted by prehypertrophic chondrocytes, a transitional phenotype between proliferation and hypertrophy (St-Jacques et al., 1999; Koyama et al., 2007; Maeda et al., 2007). Additionally, Ihh represses the onset of hypertrophic differentiation by activation of parathyroid hormone-related peptide (PTHrP) expression, thus maintaining chondrocytes in the proliferative stage (Vortkamp et al., 1996). The Gli family of transcriptional factors plays an essential role on regulating responses of chondrocytes to Ihh (Wuelling and Vortkamp, 2010). These responses rely upon the unique contributions of primary cilia (Koyama et al., 2007). Ihh, through PTHrP, prevents premature differentiation into prehypertrophic and hypertrophic phenotypes and define the number of cells that will exit the proliferative phase and differentiate further accordingly proceeding to the endochondral ossification pathway (Kobayashi et al., 2005).

FGFs acting through FGF receptor 3 (FGFR3), a tyrosine kinase receptor, serve as inhibitors of the proliferation of chondrocytes and stimulate factors of chondrocyte hypertrophy (Minina et al., 2002; Yoon et al., 2006). FGFR3 signalling can also restrain Ihh expression (Liu et al., 2002). FGFs activity is modulated by glycosaminoglycans and desulphation of glycosaminoglycans appears to limit the FGFs-induced repression of chondrocyte proliferation (Ornitz, 2005; Chuang et al., 2010). Contrary, binding of BMPs to their receptors leads to stimulation of chondrocyte proliferation and inhibition of hypertrophic differentiation. BMPs also induce the secretion of Ihh and reversely Ihh induces the secretion of various BMPs, but their interaction is not in an absolute dependent manner (Minina et al., 2001). The rate of proliferation is determined by the balance of signalling between BMPs and FGFs, which also conform the sequential transition to the hypertrophic phenotype with the proliferation rate (Minina et al., 2002).

The cartilage matrix principally consists of aggrecan and hyaluronan arranged in the fibrillar network of collagen type II, which serves as the framework for the tissue. The collagenous network provides tensile strength, while the proteoglycans contribute to the elastic properties of the tissue (Gentili and Cancedda, 2009). Cartilage matrix also involves other types of collagen to a lesser extent and other non-collagenous matrix proteins. All the components of

the cartilage matrix build an intricate network of interacting molecules, thus regulating the behaviour of chondrocytes (Heinegard, 2009). Numerous factors, such as IGF1, BMPs or TGF-β, stimulate expression and secretion of the components of the extracellular matrix, yet the role of the transcription factor Sox9 is definitely critical (Ng et al., 1997; Lefebvre et al., 2001; Yoon et al., 2005).

2.2.2. Terminal differentiation of chondrocytes and endochondral ossification

The process of endochondral ossification involves the terminal differentiation of chondrocytes to the hypertrophic phenotype, calcification of the cartilage matrix, vascular invasion, and finally ossification (Goldring et al., 2006; Fig. 4). In order to undergo hypertrophy, chondrocytes have to increase their cellular fluid volume by almost 20 times. They then stop dividing and they create hypertrophic zones, in which they are arranged in multicellular clusters, often forming a columnar structure (Mackie et al., 2011). Hypertrophic chondrocytes are present in two forms depending on their appearance: light and dark cells (Anderson, 1964; Ahmed et al., 2007).

Hypertrophic chondrocytes begin to alter the cartilage matrix and this is abetted by a shift in their secretion activity. A specific biological marker of this stage include collagen type X, a non-fibrillar collagen type, and this is accompanied by the secretion of alkaline phosphatase (ALP), matrix metalloproteinases (MMPs), and vascular endothelial growth factors (VEGFs) (Colnot and Helms, 2001; Inada et al., 2004). MMPs degrade collagen type II, which is downregulated during hypertrophy (Ortega et al., 2004). VEGFs promote the vascular invasion, which is needed in order the cartilage to be replaced by bone (Colnot and Helms, 2001; Colnot et al., 2004).

The critical transition of chondrocytes to the hypertrophic phenotype is regulated by systemic factors, such as thyroid hormones, as well (Shao et al., 2006; Wang et al., 2007). The canonical Wnt signalling pathway (Enomoto-Iwamoto et al., 2002; Chen et al., 2008), IGF1 (Wang et al., 2010) and FGFR3 (Minina et al., 2002; Ornitz, 2005) appear to be mediators of the triiodothyronine hormone (T_3)-induced chondrocyte hypertrophy. Furthermore, thyroid hormones abolish expression of PTHrP and PTHrP-R, which could be another either direct or indirect way for facilitating chondrocyte hypertrophy (Stevens et al., 2000).

Runx2 is a key transcription factor inducing hypertrophy (Otto et al., 1997; Enomoto et al., 2000; Komori, 2005). As mentioned above, PTHrP is activated by Ihh and inhibits hypertrophy of chondrocytes. PTHrP exerts its effects via suppression of expression of the Runx2 transcriptional factor (Lefebvre and Smits, 2005) and probably by Sox9, which is activated by PTHrP and indirectly reduces Runx2 expression (Huang et al., 2000). Although Ihh is considered to inhibit hypertrophy, it has been shown that in the absence of PTHrP, Ihh appears to promote chondrocyte hypertrophy (Mak et al., 2008).

Late hypertrophic chondrocytes produce and release matrix vesicles that initiate mineral deposition in skeletal tissues. They can qualitatively adjust the production of matrix vesicles and release mineralization-competent matrix vesicles rich in annexin V and alkaline phosphatase only when they are stimulated to induce mineralization (Kirsch et al., 1997; Kirsch, 2006). PHOSPHO1 phosphatase and tissue non-specific alkaline phosphatase (TNAP) both play a role on the mineralisation of cartilage matrix. PHOSPHO1 initiates mineralisation within the matrix vesicle, while TNAP progresses the mineralisation outside the boundaries of the matrix vesicle (Fedde et al., 1999; Anderson et al., 2004; Yadav et al., 2011).

The cartilage matrix remodelling and the angiogenesis induced by the activity of hypertrophic chondrocytes change the environmental stress experienced by hypertrophic chondrocytes, which eventually undergo physiological death (Goldring et al., 2006). Most hypertrophic chondrocytes seem to undergo rapid death before the ossification front (Mackie et al., 2011). Their rapid death is attributed to the apoptotic pathway, since features pertinent to apoptotic cell death were identified. Further, the apoptogenic activity of some peptides of extracellular matrix proteins was found to be powerful (Adams and Shapiro, 2002). Following apoptosis of chondrocytes, the transverse septa of the cartilage matrix enclosing them are broken down, prompting the invasion and differentiation of the cells that extend the ossification centre. Many of the vertical septa are maintained as a scaffold for bone matrix deposition (Mackie et al., 2011).

Endochondral ossification starts from all the corners of the synchondrosis (Premkumar, 2011). MMP13 and MMP9 work synergistically in a coordinated process to cleave the two major components of the cartilage matrix, collagen type II and aggrecan (Stickens et al., 2004); with cleaving of collagens being of superior importance compared to cleaving of aggrecan in regard to the normal development of the growth plate (Little et al., 2005).

Vascular invasion takes place without preceding osteoclastic activity, since angiogenesis and osteoclastogenesis were found to be dissociated *in vivo* (Deckers et al., 2002). A specialized cell type called septoclast facilitates the invading capillaries by breaking down the terminal transverse septum and providing the invasive path (Gartland et al., 2009). Osteoclasts are responsible for cartilage matrix degradation promoting the invasion of bone marrow cells or the deposition of bone matrix by osteoblasts (Mackie et al., 2008).

Factors produced by hypertrophic chondrocytes adjust the replacement of cartilage matrix by bone to the preparation of growth plate for invasion. By this means, hypertrophic chondrocytes regulate the behaviour of the invading cells. The chemoattractant high-mobility group box 1 protein (HMGB1) produced by hypertrophic chondrocytes attracts endothelial cells, osteoclasts, and osteoblasts (Taniguchi et al., 2007). Moreover, the receptor activator of NFkB ligand (RANKL) is a factor also produced by hypertrophic chondrocytes and is required for osteoclast invasion and differentiation (Kishimoto et al., 2006). RANKL production by hypertrophic chondrocytes induces formation of osteoclasts through BMP2 and Runx2 and could therefore regulate resorption of calcified matrix by osteoclasts (Usui et al., 2008).

When the proliferative potential of chondrocytes at the growth plate is exhausted, growth plate closure is initiated. Oestrogen acts indirectly by accelerating the programmed senescence of the growth plate, thus exhausting the proliferative potential of chondrocytes. Ossification of the growth plate then occurs as an aftermath (Weise et al. 2001).

2.3. The role of reactive oxygen species and antioxidants on endochondral ossification

Reactive oxygen species (ROS) are derivatives of aerobic metabolism and exposure to various natural and synthetic toxicants. Failure of cellular mechanisms to cope with elevated ROS levels can cause oxidative stress, which can lead to various deleterious phenomena, such as apoptosis, inflammatory response or ischemia. The cellular armamentarium against such a challenge includes multiple layers of antioxidant defences (Davies, 2000; Fig. 6).

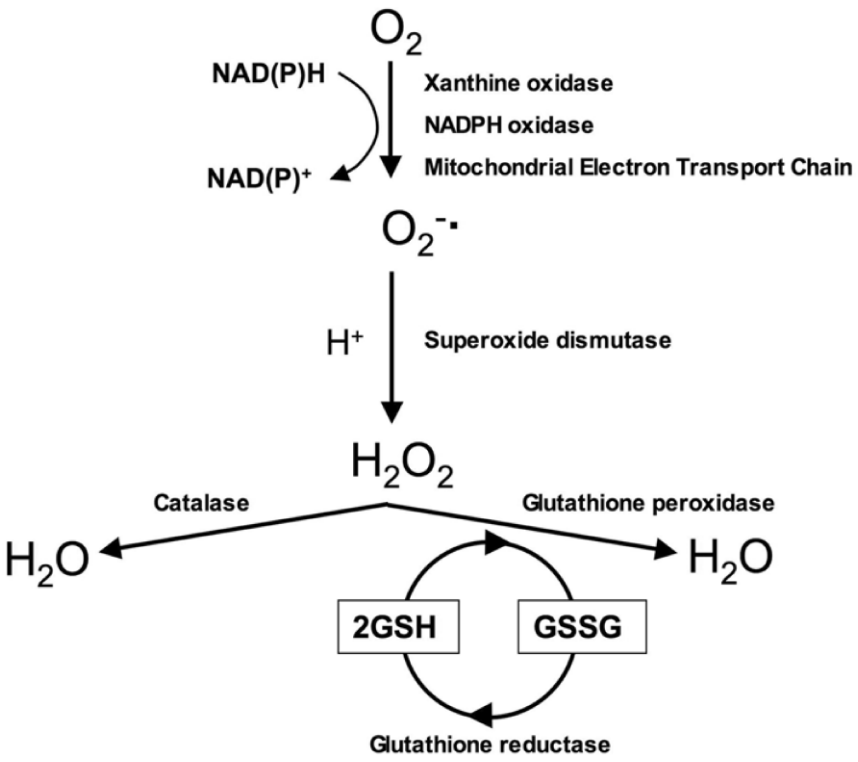

Fig. 6. Redox regulation from antioxidant enzymes (from R. J. Aitken, S. D. Roman, 2008).

However, although ROS had been better studied in regard to their cytotoxic effects, their semantic involvement in eukaryotic signal transduction is well established nowadays (Sundaresan et al., 1995; Lander, 1997; Rhee, 1999; Rhee et al., 2000; Forman et al., 2004). ROS are generally thought to act as signalling molecules through the following sequence of events: (1) in response to various stimuli they can be generated on the surface of the cells or within intracellular compartments of them, (2) after their entrance into the cytoplasm, they can react with various proteins and modulate their function, (3) the changes in protein activity induced by ROS define specific cellular responses, and (4) once the stimulus disappears, ROS are degraded and the system returns to its original state (Hurd et al., 2012).

Hydrogen peroxide (H_2O_2) can trigger various biological responses. Biological responses caused by H_2O_2 depend both on the cell type and the concentration of H_2O_2 within a cell (Chen et al., 2005; Choi et al., 2005; Sablina et al., 2005). In other words, in order the same biological response to be induced, different H_2O_2 levels are required among different types of cells, and distinct biological responses can be induced in response to low compared with high levels of H_2O_2 within a cell. Additionally, the detoxifying effect of antioxidant enzymes on

H_2O_2 seems to influence the biological response by controlling the local levels of H_2O_2 (Chang et al., 2004).

Thus, the role of antioxidant enzymes is of dual nature. It is not only restricted to the survival of cells by preventing cellular damage caused by increased H_2O_2 levels but it is also extended to the adjustment of biological response by regulating local H_2O_2 levels. In combination with the regulatory action of antioxidant enzymes, H_2O_2 can trigger various biological responses such as cell division, apoptosis, differentiation or migration (Sauer et al., 2000; Arnold et al., 2001; Cai, 2005; Li et al., 2006; Ushio-Fukai, 2006).

The involvement of ROS in regulation of cellular processes, which are vital during developmental stages, suggests that redox regulation is essential during development. Indeed, ROS have been implicated in several developmental processes such as spermatogenesis, oogenesis, and angiogenesis (Covarrubias et al., 2008). The effect of ROS on the process of endochondral ossification needs further elucidation; however, there is recent evidence supporting the crucial role of ROS during endochondral ossification.

In particular, Fragonas et al. (1998) tested the impact of ROS both on resting and hypertrophic chondrocytes, the antioxidant activity of them and the ability of ROS to induce the production of alkaline phosphatase-enriched matrix vesicles by hypertrophic chondrocytes. The extent of cell damage due to ROS treatment was estimated from free LDH activity as percent of total LDH activity of the culture. ROS promoted the damage of approximately 25% of hypertrophic chondrocytes compared with approximately 46% damage of resting chondrocytes. Catalase activity was higher in hypertrophic than resting chondrocytes but superoxide dismutase (SOD) activity was less in hypertrophic compared with resting chondrocytes. The phospholipid hydroperoxide glutathione peroxidase (Gpx4) was identified at a higher level in resting rather than hypertrophic chondrocytes. Finally, the release of matrix vesicles by hypertrophic chondrocytes demonstrated a significant increase after the treatment of chondrocytes with ROS.

Morita et al. (2007) investigated the levels of ROS in hypertrophic chondrocytes, the effect of ROS in chondrocyte differentiation process and the pathways activated by ROS during the process. It was revealed that hypertrophic chondrocytes demonstrate high levels of ROS. Furthermore, ROS initiated the inhibition of proliferating chondrocytes, while they stimulated the differentiation of proliferating to hypertrophic chondrocytes. The induction of

differentiation from proliferating to hypertrophic chondrocytes involved the activation of ERK and p38 MAPK pathways.

Kim et al. (2010) studied the contribution of several NADPH oxidases (Nox) as ROS generating sources in chondrogenesis. It was found that Nox were essential for chondrocyte differentiation as contributing to the elevation of intracellular ROS levels. Nox1 and Nox2 were increased during the time course of differentiation, whereas Nox4, although relative high initially, was decreased afterwards. The depletion of both Nox2 and Nox4, but not Nox1, resulted in a cessation of ROS generation and chondrocyte differentiation. Additionally, the depletion of Nox2 and Nox4 induced apoptosis and inhibited the accumulation of proteoglycans.

2.4. Glutathione peroxidase 1

Glutathione peroxidases (Gpxs) belong to the broad family of selenium- or cysteine-containing proteins. Glutathione peroxidase 1 (Gpx1) was the first to be described in 1957, as an enzyme that protects hemoglobin of erythrocytes from oxidative breakdown (Mills, 1957). Later much more types of Gpxs were discovered not only in mammalian vertebrates, but in non-mammalian vertebrates as well. Under the general term "glutathione peroxidases" is considered to be a wide range of proteins that demonstrate sequence homology; such as Gpx1, Gpx2, Gpx3, Gpx4, and Gpx5. Although selenium-containing Gpxs were detected in non-mammalian vertebrates as well, the vast majority of Gpxs are cysteine-dependent in the former form of life (Tosatto et al., 2008), whereas mammalian Gpxs contain selenocysteine, which is the main form of selenium metabolism *in vivo* (Sun et al., 2011).

Gpx1 is a widely distributed intracellular protein; ubiquitously present in all tissues. It functions both in cytosol and mitochondria and its expression is higher in cytosol (70%) than in mitochondria (20-30%). It demonstrates a tetrameric structure with four identical subunits, each of which containing one atom of selenium (Se) bound as selenocysteine (Sec) moiety at the active site of the enzyme (Ursini and Maiorino, 2004; Rahman and Biswas, 2006). The Sec moiety is surrounded by the Gln, Asn, and Trp residues forming the catalytic tetrad that is conserved for Gpxs and normally located at the N-terminal end (Lu and Holmgren, 2009; Flohé and Brigelius-Flohé, 2012).

Sec is the redox-active moiety (peroxidatic Sec, UP) because in catalysis undergoes sequential conversions from reduced into oxidized form and then to a mixed selenodisulfide, and finally to the reduced form again (Rocher et al., 1992; Kulinsky and Kolesnichenko, 2009). Oxidized and reduced substrates bind sequentially at the active site of Gpx1 in order the general reactions to occur: $2GSH + H_2O_2 \rightarrow GSSG + 2H_2O$ and $2GSH + ROOH \rightarrow GSSG + ROH + H_2O$ (Kulinsky and Kolesnichenko, 2009; Fig. 7).

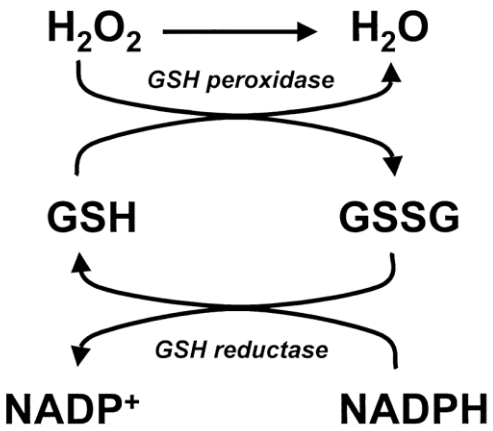

Fig. 7. Reduction cycle of Gpx1 (adapted from W. Dröge, 2002).

Specificity towards oxidized substrates for Gpx1 includes a wide range of organic hydroperoxides, such as H_2O_2, almost all aliphatic and cyclic organic peroxides (ROOH), polyunsaturated fatty acids, certain steroids, prostaglandin F2α (PGF2α), and prostaglandin G2 (PGG2) (Kulinsky and Kolesnichenko, 2009). Lipid hydroperoxides cannot be reduced from Gpx1 unless they are soluble; thus, they have to be pre-treated with phospholipase A2. This substrate specificity might be explained by the structure of the enzyme due to which the access of large substrates appears to be limited to the peroxidatic moiety at the active site (Toppo et al., 2009). On the other hand, Gpx1 demonstrates high specificity towards reduced substrates. Glutathione (GSH) is the only naturally occurring thiol that predominates in the cell and efficiently reduces Gpx1 (Kulinsky and Kolesnichenko, 2009; Toppo et al., 2009).

3. Materials and methods

3.1. Materials

The materials used in this study and their providers are listed in Tables 1-11 according to experimental procedure.

Table 1. Consumables and their providers.

Product	**Provider**
6-well culture plates	Sarstedt AG & Co
96-well qRT-PCR plates	Biozym Scientific GmbH
75-ml tissue culture flasks	Sarstedt AG & Co
Gloves	Bio World Medical AG
Cryotubes	Carl Roth GmbH & Co KG
Pasteur pipettes (5, 10, and 25 ml) (glass)	VWR International
Pasteur pipettes (5, 10, and 25 ml) (plastic)	Sarstedt AG & Co
Cell-culture dishes	BD Falcon
Forceps	Carl Roth GmbH & Co KG
Pipettes „Eppendorf Research Plus“ 0,1-2,5 µl	Eppendorf AG, Hamburg
Pipettes „Eppendorf Research Plus“ 0,5-10 µl	Eppendorf AG, Hamburg
Pipettes „Eppendorf Research Plus“ 2-20 µl	Eppendorf AG, Hamburg

Pipettes „Eppendorf Research Plus“ 10-100 µl	Eppendorf AG, Hamburg
Pipettes „Eppendorf Research Plus“ 100-1000 µl	Eppendorf AG, Hamburg
Electronic pipette „Easypet“	Eppendorf AG, Hamburg
Pipet tips	Kisker Biotech GmbH & Co KG
Reaction vessels (0.2, 0.5, 1, 1.5, and 2 ml)	Kisker Biotech GmbH & Co KG
Reaction vessels (25 and 50 ml)	Sarstedt AG & Co
Optical adhesive films „BZO Seal Film”	Biozym Scientific GmbH
Scalpels	Aesculap AG
Centrifuge tubes (50 ml)	Sarstedt AG & Co
Microscope slides	Thermo Scientific
Slide Staining System „EasyDip”	Ted Pella, Inc.
Cover slips	Engelbrecht Medizin- und Labortechnik GmbH
Syringe filters	Sartorius

Table 2. Laboratory equipment and corresponding manufacturers.

Name	**Manufacturer**
Autoclave „SystecVX-150“	Systec GmbH
CO_2-Incubator	Binder
Ice machine „ZBE 30-10“	ZIEGRA Eismaschinen GmbH
Freezer	Robert Bosch GmbH
Fridge „Liebherr CN 3556“	Liebherr

Microscope „Olympus IX 50“	Olympus Europa Holding GmbH
Real-Time PCR cycler „Eppendorf Realplex“	Eppendorf AG, Hamburg
Shaker	Biometra
Spectrophotometer „GENESYS 10S UV –VIS“	Thermo Scientific
Laminar flow cabinet „Hera Safe KS“	Haereus Holding GmbH
Liquid nitrogen storage tank (N2-tank)	Tec Lab GmbH
Thermal cycler „Doppio 2.48 well“	VWR International
Vortex „Genie 2“	Scientific Industries Inc. Bohemia NY.
Analytical balance „KernABJ“	Kern & Sohn GmbH
Water bath	Köttermann
Coulter counter	Beckman Coulter
Centrifuge „Eppendorf Centrifuge 5804 R“	Eppendorf AG, Hamburg
Centrifuge „Haereus Fresco 17 Centrifuge“	Haereus Holding GmbH
Microtome HM 350	MICROM GmbH
Paraffin water bath	Medax Nagel GmbH
Cooling plate	KUNZ INSTRUMENTS AB
Fume cupboard	WALDNER Laboreinrichtungen GmbH & Co. KG
Gel documentation system “GenoPlex”	VWR International
Gel electrophoresis system	VWR International
Semi-dry blotter	VWR International

Table 3. Materials for the cell culture.

Product	**Provider**
ATDC5 cell line	Sigma-Aldrich
1:1 DMEM and Ham's F-12 medium	Sigma-Aldrich
Fetal calf serum	PAN-Biotech GmbH
Antibiotics and antimycotics	PAA Laboratories GmbH
Human transferrin	Sigma-Aldrich
Sodium selenite	Sigma-Aldrich
Human insulin	PromoCell GmbH
Ascorbic acid	Sigma-Aldrich
Trypsin-EDTA	Gibco
PBS buffer	Sigma-Aldrich
Isotonic-II	Carl Roth GmbH & Co KG

Table 4. Materials for the RNA isolation.

Product	**Provider**
peqGOLD TriFast reagent	PEQLAB Biotechnologie GmbH
Chloroform	Merck Chemicals GmbH
Isopropanol	Merck Chemicals GmbH
Ethanol	Carl Roth GmbH & Co KG
DEPC-water	Carl Roth GmbH & Co KG

Table 5. Materials for the cDNA.

Product		**Provider**
M-MLV Reverse Transcriptase, 50.000u	M-MLV reverse transcriptase	Promega Corporation
	M-MLV RT buffer, 5x	

Table 6. Materials for the qRT-PCR.

Product		**Provider**
Primers	Polr2a	Eurofins MWG Operon
	Gpx1	
	Col2a1	
	Col10a1	
SYBR Green JumpStart Taq ReadyMix		Sigma-Aldrich

Table 7. Materials for the stains.

Product	**Provider**
Acetic acid	Merck Chemicals GmbH
Alcian blue 8 GS	Waldeck GmbH & Co KG
Methanol	Fisher Scientific
Alizarin red S	Carl Roth GmbH & Co KG

Table 8. Materials for the immunohistochemistry.

Product	**Provider**
Xylene	Carl Roth GmbH & Co KG
Ethanol	Carl Roth GmbH & Co KG

Tris-EDTA buffer	Tris	Sigma-Aldrich
	Hydrogen chloride	Merck Chemicals GmbH
	EDTA	AppliChem GmbH
	Tween 20	Carl Roth GmbH & Co KG
DAKO peroxidase blocking reagent		Dako
Gpx1 primary antibody		Abcam
Secondary antibody		Rockland Immunochemicals
Diaminobenzidine chromogenic substrate		Dako

Table 9. Materials for the overexpression and knockdown of Gpx1.

Product		**Provider**
Phusion high-fidelity PCR kit	Phusion DNA polymerase	New England Biolabs
	Deoxynucleotide solution	
	Phusion HF buffer	
	Phusion GC buffer	
	$MgCl_2$ solution	
	Kontroll-Lambda template	
	1.3 and 10 kb primers	
	DMSO	
	Quick-Load DNA marker	

QIAquick gel extraction kit	QIAquick spin columns	Qiagen
	Buffer	
	Collection tubes	
pcDNA 3.1 Directional TOPO Expression Kit	pcDNA 3.1D/V5-His-TOPO	Invitrogen
	dNTP mix	
	Salt solution	
	Sterile water	
	T7 sequencing primer	
	BGH reverse sequencing primer	
	Control PCR template	
	Control PCR primers	
	Expression plasmid	
	S.O.C. medium	
	TOP10 cells	
	pUC19 control DNA	
NucleoBond Xtra midi plus	Buffer RES	MACHEREY-NAGEL
	Buffer LYS	
	Buffer NEU	
	Buffer EQU	
	Buffer WASH	
	Buffer ELU	

	RNase A	
	NucleoBond Xtra midi columns and column filters	
	NucleoBond finalizers	
	30 ml syringes	
	1 ml syringes	
	Buffer TRIS	
LB medium		Carl Roth GmbH & Co KG
Serum-free medium		Sigma-Aldrich
TurboFect transfection reagent		Thermo Scientific
Trilencer-27 siRNA kit	Gene-specific siRNA duplexes	OriGene
	Universal scrambled negative control siRNA duplex	
	Rnase free siRNA duplex re-suspension buffer	

Table 10. Materials for western blotting.

Product		**Provider**
CelLytic M reagent		Sigma-Aldrich
Stacking and running SDS-gel	Acrylamide mix	Carl Roth GmbH & Co KG
	Tris	Sigma-Aldrich

	SDS	Carl Roth GmbH & Co KG
	APS	Carl Roth GmbH & Co KG
	TEMED	Carl Roth GmbH & Co KG
	Bromophenol blue	Sigma-Aldrich
SDS-running buffer	Tris	Sigma-Aldrich
	SDS	Carl Roth GmbH & Co KG
	Glycine	Carl Roth GmbH & Co KG
Transfer buffer	Tris	Sigma-Aldrich
	Glycine	Carl Roth GmbH & Co KG
	Methanol	Fisher Scientific
	SDS	Carl Roth GmbH & Co KG
TBS-T buffer	Tris	Sigma-Aldrich
	NaCl	Carl Roth GmbH & Co KG
	HCl	Fisher Scientific
	Tween 20	Carl Roth GmbH & Co KG
Roti-Load 1, 4x		Carl Roth GmbH & Co KG
PVDF membrane		Carl Roth GmbH & Co KG
Filter papers		GE Healthcare Europe GmbH
Gpx1 primary antibody		Abcam
Secondary antibody		Rockland Immunochemicals
Powdered milk		Carl Roth GmbH & Co KG

Table 11. Materials for the experiments on apoptosis.

Product		**Provider**
Hydrogen peroxide		Carl Roth GmbH & Co KG
Annexin V-FITC apoptosis detection kit I	Annexin V-FITC	BD Pharmingen
	Propidium iodide staining solution	
	Annexin V binding buffer	

3.2. Methods

3.2.1. Culture conditions

The mouse embryonal teratocarcinoma-derived ATDC5 cell line was used, which is a suitable *in vitro* model to simulate chondrogenic differentiation analogous to that occurring during endochondral ossification *in vivo* (Atsumi et al., 1990; Yao and Wang, 2013). Cells were thawed and seeded in 75ml-culture flasks. The medium consisted of 1:1 mixture of DMEM and Ham's F-12 supplemented with 5% FCS (fetal calf serum) and 1% AA (antibiotics and antimycotics). Upon confluence observed with an optical microscope, cells were subcultured and the resulting passages were between 15th and 19th. The passaging of cells was done according to protocol in Table 12.

Cells were inspected with light microscopy every day to confirm proper proliferation and absence of contamination. The protocol for determining the number of cells is presented in Table 13.

The culture medium differed across experiments. To observe the temporal expression pattern of Gpx1 during chondrogenic differentiation, cells received the maintenance medium comprising 1:1 mixture of DMEM and Ham's F-12 supplemented with:

- 5% FCS
- 1% AA

- 10 μg/ml human transferrin
- 3×10^{-8} M sodium selenite

Table 12. Protocol for passaging the cells.

1	Removing the culture medium and washing cells with PBS buffer
2	Dissociating of cell contacts with 1, 0.2, and 0.4 ml trypsin for 75ml-culture flasks, 6-well plates, and cell-culture dishes respectively
3	Incubation for 4 min at 37 °C in a CO_2 incubator
4	Addition of culture medium at least twice the amount of trypsin for inhibiting trypsin
5	Transferring to tubes
6	Sedimentation of cells by centrifugation at 1200 rpm for 5 min
7	Removal of supernatants and resuspension of pellets in medium
8	Determination of cell number with a Coulter counter

Table 13. Protocol for determining the number of cells.

1	Filling of 10 ml Isotonic-II in a plastic measuring vessel
2	Adding 100 μl of the cell suspension and uniformly mixing by repeated shaking
3	Blank measurement with the Coulter counter according to the manufacturer's instructions (must be maximum 1% of the determined cell number / ml amount)
4	Determination of cell number in the wells (cell number / ml)
5	Calculating the required volume of cell suspension for the desired number cells
6	Seeding and recultivation of the cells

For inducing chondrogenesis from the fifth day of culture (corresponding to day 0 of the measurements) and over the following 21 days, the differentiation medium was prepared by additionally supplementing the maintenance medium with (Altaf et al., 2006):

- 10 µg/ml human insulin
- 20 mg/ml ascorbic acid

The aforementioned differentiation medium was also used for the knockdown experiments. For the overexpression experiments the medium was:

- 5% FCS
- 1% AA
- 10 µg/ml human transferrin
- 100 nM sodium selenite

The medium was replaced every other day, unless otherwise stated, and cell cultures were maintained at 37 °C under a humidified atmosphere of 5% CO_2.

3.2.2. Isolation of RNA

After washing cells with PBS buffer, 1 ml peqGOLD TriFast reagent was applied per well and left for 5 min. The solution was transferred to tubes, where 200 µl chloroform were added. The mixture was well vibrated and left until the separation of aqueous and organic phase. The mixture was then centrifuged at 4 °C and 14000 rpm for 10 min. The aqueous phase was removed to new tubes, where 400 µl isopropanol was pipetted. Samples were incubated at 4 °C for 10 min, followed by centrifugation at 4 °C and 14000 rpm for 15 min. Supernatants were removed and pellets were washed twice with 1 ml of 70% ethanol followed by centrifugation at 4 °C and 7500 g for 5 min. Pellets were left to dry for 10 min and RNA was dissolved in 25 µl DEPC-water. Samples were immediately placed on ice for subsequent quantification of RNA.

A spectrophotometer was used for quantifying RNA at wavelengths of 260 nm and 280 nm. Whenever the concentration of nucleic acid in the samples was above 600 ng/µl, additional amount of DEPC-water was added. The purity of the samples was defined by the

OD260/OD280 ratio and samples were admissible whenever the ratio was above 1.8. After determining RNA concentration and purity, samples were stored at -80 °C until further handling.

3.2.3. Reverse transcription

RNA was transcribed to cDNA with the M-MLV Reverse Transcriptase. All the tubes were kept on ice throughout the process. Samples contained the following:

- 1 µg RNA template
- 4 µl M-MLV Reaction Buffer, 5x
- 1 µl Oligo(dT)
- 1 µl Random Hexamer
- 1 µl dNTP Mix, 10 mM
- RNase-free H_2O, summing up to a volume of 20 µl

Samples were then incubated at 70 °C for 3 min. Afterwards, the following were added:

- 1 µl RNase Inhibitor
- 1 µl M-MLV Reverse Transcriptase

Samples were finally incubated at 37 °C for 60 min and at 95 °C for 2 min. They were then kept at -20 °C until further use.

3.2.4. Quantitative Real-Time PCR

Four primers were used for this study: polymerase II (Polr2a), glutathione peroxidase 1 (Gpx1), Collagen type II (Col2a1), and collagen type X (Col10a1). The expression of Polr2a was set as the endogenous control, while Col2a1 and Col10a1 were chondrogenic gene markers corresponding to different stages of differentiation. Col2a1 is a well-established marker for the initial differentiation of chondrocytes, while Col10a1 is a marker for the

terminal differentiation (van der Earned et al., 2003; Mackie et al., 2008). Both of them have also been identified at the spheno-occipital synchondrosis (Römer et al., 2010). Primers are presented in Table 14.

Table 14. Primers for the qRT-PCR used in this study.

Name	**Symbol**		**Primer sequence**	**Accession number**	**Provider**
Polymerase (RNA) II (DNA directed) polypeptide A	Polr2a	F	5'-aatccgcatcatgaacagtg-3'	NM_009089.2	Eurofins MWG Operon
		R	5'-tcatccattttatccaccacct-3'		
Glutathione peroxidase 1	Gpx1	F	5'-tttcccgtgcaatcagttc-3'	NM_008160	Eurofins MWG Operon
		R	5'-tcggacgtacttgagggaat-3'		
Collagen, type II, alpha 1	Col2a1	F	5'-cggtcctacggtgtcagg-3'	NM_031163.3	Eurofins MWG Operon
		R	5'-ttatacctctgcccattctgc-3'		
Collagen, type X, alpha 1	Col10a1	F	5'-gcatctcccagcaccaga-3'	NM_009925.4	Eurofins MWG Operon
		R	5'-ccatgaaccagggtcaagaa-3'		

F: forward primer; R: reverse primer

All the material was kept on ice throughout the process. All qRT-PCR reactions were performed in triplicates and for each pair of primers negative controls were included. The reaction mix consisted of the following:

- 5.25 µl DEPC-H_2O
- 7.5 µl SYBR Green JumpStart Taq ReadyMix
- 0.375 µl forward primer (10 pmol/µl)

- 0.375 µl reverse primer (10 pmol/µl)
- 1.5 µl cDNA (10x diluted)

The reaction mix was pipetted in 96-well plates, which were covered with an optical adhesive film. Cycling conditions were as follows:

- Heat up and initial denaturation at 95 °C for 5 min
- Denaturation of the double stranded DNA at 95 °C for 10 sec
- Annealing of primers at 60 °C for 8 sec
- Elongation and fluorescence-point measurement at 72 °C for 8 sec

The amplification reaction was repeated for 45 cycles and an extra step of melting curve was always included, to insure the specificity of primers. The melting curve step consisted of the following:

- Initial denaturation at 95 °C for 15 sec
- Annealing of primers at 60 °C for 15 sec
- Rise of the temperature from 60 °C to 95 °C within 20 min with ongoing measurement of the fluorescence
- Maintenance of the temperature at 95 °C for 15 sec

In order to be statistically analysed, data were normalized against the endogenous control according to the formula:

$$\Delta Ct = Ct_{\text{endogenous control}} - Ct_{\text{gene of interest}}$$

For this purpose, the mean of the triplicates was always considered, if the standard deviation did not exceed 0.60. Otherwise, the outlier was excluded and the mean of the two remaining identical wells was taken into account. For presenting the data, the mRNA levels were normalized against the endogenous control and logarithmic scaled on the base of 2. They are presented as individual data points (Schmittgen and Livak, 2008): $2^{\Delta Ct}$.

3.2.5. Stains

For visualizing the process of chondrogenic differentiation, Alcian blue and Alizarin red stains were used. Alcian blue stain reveals the formation of glycosaminoglycans in cartilage nodules (Shukunami et al., 1996). Cells were rinsed with 1 ml PBS buffer per well. They were then fixed with 1 ml of 0.1% glutaraldehyde and PBS buffer solution per well at room temperature for 20 min. Thereafter, cells were washed twice with Millipore water and left with 1 ml Alcian blue stain solution at room temperature for 30 min. Alcian blue stain solution consisted of 0.0125 g Alcian blue 8 GS, 0.375 ml of 10% acetic acid (pH = 2.5), and 0.875 ml distilled water per well. After that, cells were rinsed under warm running tap water for 2 min. Finally, cells were washed with 1 ml Millipore water and inspected microscopically.

Alizarin red stain shows the mineralization of the extracellular matrix (Shukunami et al., 1997). Cells were washed with 1 ml PBS buffer per well and then fixed with 500 µl methanol at room temperature for 10 min. Subsequently, cells were washed with 1 ml distilled water per well and 500 µl Alizarin red S were applied and left at room temperature for 2 min. After removing Alizarin red S, cells were rinsed three times with 1 ml tap water and inspected microscopically. Photos for both stains were taken with an optical microscope.

3.2.6. Immunohistochemistry

The spheno-occipital synchondrosis from eight 10-days old male Wistar rats (Fig. 5, 8) was isolated and the corresponding paraffin-embedded tissue blocks were provided by Dr. Jens Weingärtner (Institute of Anatomy and Cell Biology, Ernst Moritz Arndt University of Greifswald). The paraffin-embedded tissue blocks were sectioned at 2 µm thickness with a microtome and sections were floated in a water bath. After transferring sections onto glass slides, they were left to dry overnight.

On the day of use, samples were deparaffinized by incubating at 70 °C and immersing in xylene for 3 min. Then, tissues were hydrated in 95%, 70%, and 50% ethanol for 5, 5, and 10 min respectively. To unmask the antigenic epitope, Tris-EDTA buffer (10 mM Tris, 1 mM EDTA, 0.05% Tween 20, pH 9.0) antigen retrieval was performed at 95 °C in a pre-heated

water bath for 2 h. Blocking of non-specific binding sites was done with DAKO Peroxidase Blocking Reagent for 10 min at room temperature. 100 µl anti-Gpx1 primary monoclonal antibody (1:250; ab108427, Abcam) were then applied for 1 h followed by 100 µl goat anti-rabbit antibody conjugated with horseradish peroxidase (611-1302, Rockland Immunochemicals) for 30 min. Diaminobenzidine chromogenic substrate for antibody detection was applied for 3 min and samples were additionally counterstained in hematoxylin for 2 min. Tissue slides were dehydrated in ethanol and cleared in xylene before coverslipping. Negative controls included sections that were incubated without the primary or secondary antibodies.

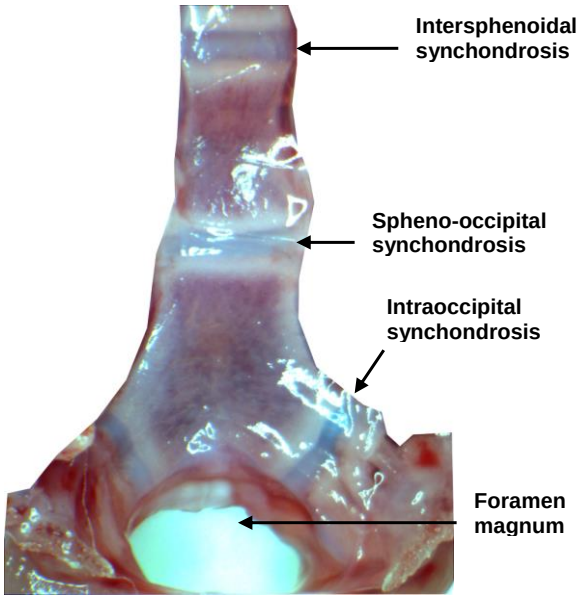

Fig. 8. Cranial base of 10 days old Wistar rat dissected for immunohistochemistry, Magn. ×10 (from V. Koretsi et al., 2015).

Photographs of the immunostained sections were analysed at ×200 magnification factor. Immunoreactivity of Gpx1 was semiquantitatively determined by two independent observers and the agreement was assessed according to Landis and Koch (1977). The following grades were assigned to resting, proliferating, and hypertrophic zones:

- Grade 0, no immunoreactivity
- Grade 1, weak immunoreactivity (less than 25% of the cells)
- Grade 2, moderate immunoreactivity (25-50% of the cells)
- Grade 3, strong immunoreactivity (50-75% of the cells)
- Grade 4, very strong immunoreactivity (more than 75% of the cells)

Multiple sections were analysed per specimen and the median of replicates was then considered. Repeatability was assessed by analysing randomly selected photographs with an interval of a week.

3.2.7. Overexpression and silencing of Gpx1

The expression of Gpx1 was transiently manipulated in ATDC5 chondrogenic cell line. For the overexpression experiments, Gpx1 was amplified from the cDNA of ATDC5 cells with the Phusion High-Fidelity PCR Kit. The reaction mixture comprised 4 µl 5xPCR-buffer, 0.4 µl dNTPs, 1 µl of 1:10 diluted cDNA containing 1 µg RNA, 1 µl of each primer, 0.2 µl DNA polymerase, and 12.4 µl H_2O. The forward and reverse primers were 5'-caccatgtgtgctgctcggctct-3' and 5'-ccttaggagttgccagactgc-3' respectively. Cycling conditions were 98 °C for 30 sec, followed by 30 cycles at 98 °C for 10 sec, 60 °C for 30 sec and 72 °C for 30 sec, and a final extension of 72 °C for 5 min. Extraction and purification of the amplificates was done with QIAquick Gel Extraction Kit. Specifically, 3 volumes of QG buffer were mixed with 1 volume of samples and the samples were then centrifuged with the QIAquick Spin Column for 60 sec. The flow-through was discarded and samples were washed with 0.75 ml PE buffer. Samples were again centrifuged for 1 min at maximum speed. The QIAquick Spin Column was placed into a clean microcentrifuge tube. Finally, 30 µl elution buffer were added, samples were left for 1 min, and they were then centrifuged for 1 min. DNA was sequenced with Eurofins MWG Operon and the cloned sequence was found to be identical to the murine Gpx1 (NM_008160).

The mammalian expression vectors pcDNA 3.1D/V5-His-TOPO were transformed in Escherichia coli and the plasmid DNA was purified with NucleoBond Xtra Midi Plus. The culture stemming from diluting the starter culture 1:1000 into LB medium was left to grow overnight. After harvesting bacterial cells, they were pelleted by centrifugation and the supernatant was discarded. Cells were resuspended in Resuspension Buffer RES + RNase A and the LYS buffer was added to the suspension at room temperature for 5 min. Then the EQU buffer was applied to the NucleoBond Xtra Column followed by NEU buffer for neutralization. After applying the lysate, the column filter and column were washed with EQU buffer and the column filter was discarded. The column was washed with WASH buffer and the plasmid DNA was eluted with ELU buffer. Subsequently, isopropanol for precipitating the eluted plasmid DNA was added and the samples were centrifuged. The supernatant was discarded and 70% ethanol was added to the DNA pellet. After centrifuging, ethanol was removed and the pellet was left to dry. To reconstitute DNA, pellet was dissolved in Tris-EDTA buffer. Nucleic acid concentration and purity were determined by spectrophotometry.

ATDC5 cells were transfected with Gpx1 or LacZ (control) plasmids in TurboFect Transfection Reagent. Twenty four hours prior to transfection, 5×10^5 cells were seeded with 4 ml medium in cell-culture dishes. 8 µg of DNA were diluted in 800 µl of serum-free DMEM medium per cell-culture dish and 12 µl of TurboFect were added to the diluted DNA per cell-culture dish. The mixture was incubated at room temperature for 20 min and then 800 µl of it were added to each cell-culture dish dropwise. Finally, cell-culture dishes were gently rocked and incubated at 37 °C in a CO_2 incubator for the next 72 h. The overexpression of Gpx1 in ATDC5 cells was confirmed with qRT-PCR.

To knockdown Gpx1, siRNA transfections were performed with Trilencer-27 siRNA kit. 5×10^5 ATDC5 cells were seeded with 4 ml medium in cell-culture dishes 24 h prior to transfection and transfected with 5 nM Gpx1-siRNA and scrambled RNA as negative control (SR405153, OriGene). The siRNA was diluted to 5 µM using the sterilized duplex buffer supplied with the kit. Then, 5 µl of the diluted 5 µM siRNA were mixed with 320 µl serum-free medium in tubes. 20 µl siTran were diluted with 240 µl serum-free medium and the dilution was added to the aforementioned siRNA solution. The mixture was incubated at room temperature for 10 min. The mixture was finally transferred to the cell-culture dishes and those were incubated at 37 °C in a CO_2 incubator for the next 72 h. Knockdown of Gpx1 was confirmed with qRT-PCR.

3.2.8. Western blotting

Western blot was performed to ensure protein expression after manipulating Gpx1 levels in ATDC5 cells. Cells were trypsinized and counted as previously described. They were subsequently centrifuged at 4 °C and 14000 rpm for 10 min. Supernatants were removed and pellets were resuspended in CelLytic M reagent (125 µl / 10^6 cells). They were then incubated on a shaker at room temperature for 15 min. After transferring the samples into 1ml-tubes, they were centrifuged at 4 °C and 16000 rpm for 15 min. The protein-containing supernatants were transferred to new chilled tubes and samples were stored at -70 °C until further handling.

The stacking and 15% running SDS-gel were prepared according to Table 15. The solution of the running SDS-gel was inserted into electrophoresis chamber. After its polymerization, the stacking gel was applied onto it along with the combs to form the slots. During polymerization of the stacking gel, samples were heated at 99 °C for 5 min to denature the proteins.

Table 15. Composition of stacking and 15% running SDS-gel.

Ingredients	**stacking gel**	**15% running SDS-gel**
H_2O	1.4 ml	1.1 ml
Acrylamide mix (30%)	330 µl	2.5 ml
Tris	250 µl (1 M; pH 6.8)	1.3 ml (1.5 M; pH 8.8)
SDS (10%)	20 µl	50 µl
APS (10%)	20 µl	50 µl
TEMED	2 µl	2 µl
Bromophenol blue (0.5%)	0.6 µl	-
Total volume	2.0226 ml	5.002 ml

The solution containing 6 µg protein in 16 µl H_2O and 4 µl Roti-Load 1, 4x was pipetted into the slots and the electrophoresis chamber was filled with SDS-running buffer, 1x (Table 16). A voltage of 80 V for 30 min was initially applied to the chamber and then the voltage was increased at 120 V for 90 minutes for separating the proteins.

Table 16. Composition of SDS-running buffer, 1x.

Ingredients	**Amount for SDS-running buffer, 10x**
Tris (pH 8.5)	30 g
SDS	10 g
Glycine	144 g
Dissolving in distilled H_2O and topping up to 1000 ml distilled H_2O	
SDS-running buffer, 1x: 100 ml SDS-running buffer, 10x + 900 ml distilled H_2O	

Methanol was subsequently applied to the polyvinylidene difluoride membrane (PVDF membrane) for 30 sec and the running SDS-gel was placed onto the PVDF membrane. Both of them were placed between several layers of filter paper saturated with transfer buffer, 1x. Care was taken to avoid air bubbles. The composition of the transfer buffer, 1x is presented in Table 17.

The stack was then placed onto a semi-dry blotter in direct contact with electrodes and the transfer of proteins to the PVDF membrane took place with 80 mA for 60 min. Before applying antibodies, blocking of non-specific binding sites was done with a solution containing 5% milk and 95% TBS-T, 1x prepared as presented in Table 18. The membrane was then incubated overnight at 4 °C on a shaker.

Table 17. Composition of the transfer buffer, 1x.

Ingredients	**Amount for transfer buffer, 1x**
Tris	58 g
Glycine	29 g
SDS (10%)	4 g
Dissolving in distilled H_2O and topping up to 1000 ml distilled H_2O, resulting in transfer buffer, 10x	
Transfer buffer, 10x	100 ml
Methanol	200 ml
Topping up to 1000 ml distilled H_2O, resulting in transfer buffer, 1x	

Table 18. Composition of TBS-T, 1x.

Ingredients	**Amount for TBS-T, 10x**
Tris	24.23 g
NaCl	80.06 g
distilled H_2O	800 ml
Setting the pH to 7.5 with HCl (approximately 150 ml)	
Topping up to 1000 ml distilled H_2O	
For TBS-T, 1x: 100 ml TBS-T, 10x + 899 ml distilled H_2O + 1 ml Tween 20	

The Gpx1 primary antibody (1:2000, ab108427, Abcam) was applied in a solution of 0.5% milk and 99.5% TBS-T and incubated at room temperature for 90 min on a shaker. The membrane was then washed three times with TBS-T, each time for 10 min at room temperature on a shaker. Secondary antibody (1:5000, 611-1302, Rockland Immunochemicals) dissolved in the same solution was applied and incubated at room temperature for 60 min. The membrane was finally washed twice with TBS-T for 10 min,

once with PBS buffer for 5 min, and once with TBS-T for 5 min. The detection through chemiluminescence was carried out with the gel documentation system “GenoPlex” and its corresponding software “GenoSoft”.

3.2.9. Exposure to H_2O_2 and apoptosis assay

After incubating for 72 h, transfected cells were treated with exogenous H_2O_2 and the quantity of apoptotic cells was determined. After removing the old medium, ATDC5 cells were provided with 4 ml of fresh medium additionally supplemented with 250 µM H_2O_2. Cells were incubated at 37 °C in a CO_2 incubator for 6 h, after which the percentage of cells undergoing apoptosis was assessed by flow cytometry with the Annexin V-FITC Apoptosis Detection Kit I. The medium was collected and centrifuged resulting in the formation of pellets, while adherent cells were trypsinized. Both resulting pellets were then united and quantified. For the staining, cells were initially washed twice with cold PBS buffer and then resuspended in binding buffer, 1x. 100 µl of the solution were transferred to tubes, where 5 µl FITC Annexin V and 5 µl PI (propidium iodide) were added. Tubes were gently vortexed and incubated at room temperature in the dark for 15 min. Finally, 400 µl of binding buffer, 1x were supplied to each tube and samples were analysed with a flow cytometer within an hour. The settings were the following: FSC = 5 V, SSC = 350 V, FITC = 335 V, and PerCP-Cy5-5 = 395 V.

3.2.10. Statistical analysis

Statistical evaluation was performed using the SPSS programme, version 20.0 for Windows (SPSS Inc., Chicago, USA). All the statistical tests were two-sided at a level of significance $p \leq 0.05$. Data on the temporal expression pattern and immunohistochemical quantification of Gpx1 were compared for significance with the Friedman’s two-way analysis of variance by ranks. If there was a total significance level of $p \leq 0.05$, paired multiple comparisons were undertaken with the Wilcoxon test at an adjusted p value according to the correction of Bonferroni. Data on apoptosis were analysed with Welch’s ANOVA and multiple comparisons were undertaken with the Games-Howell test. Descriptive statistics are presented

as mean and standard error for continuous data, whereas median and interquartile range are given for ordinal data.

For the statistical analysis of the apoptosis assay, each experimental sample was calculated relative to its control and expressed as a ratio. Specifically, the value of each control sample was equated to 1 and the value of the corresponding experimental sample was converted accordingly.

4. Results

4.1. Chondrogenic differentiation of ATDC5 cell line

4.1.1. Stains

The chondrogenic differentiation of ATDC5 cells was determined with the stains Alcian blue and Alizarin red. The production of glycosaminoglycans (Fig. 9) and the calcification of extracellular matrix (Fig. 10) became intense with the course of differentiation. Furthermore, the formation of cartilage nodules is visible.

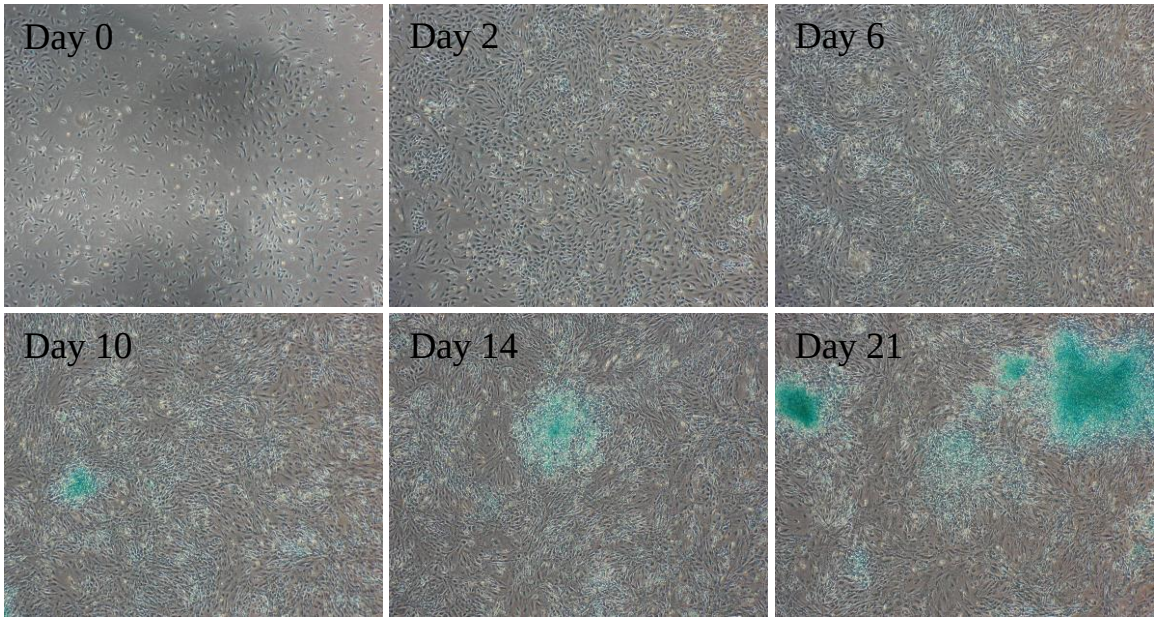

Fig. 9. Alcian blue stain for the visualization of glycosaminoglycans, Magn. ×40.

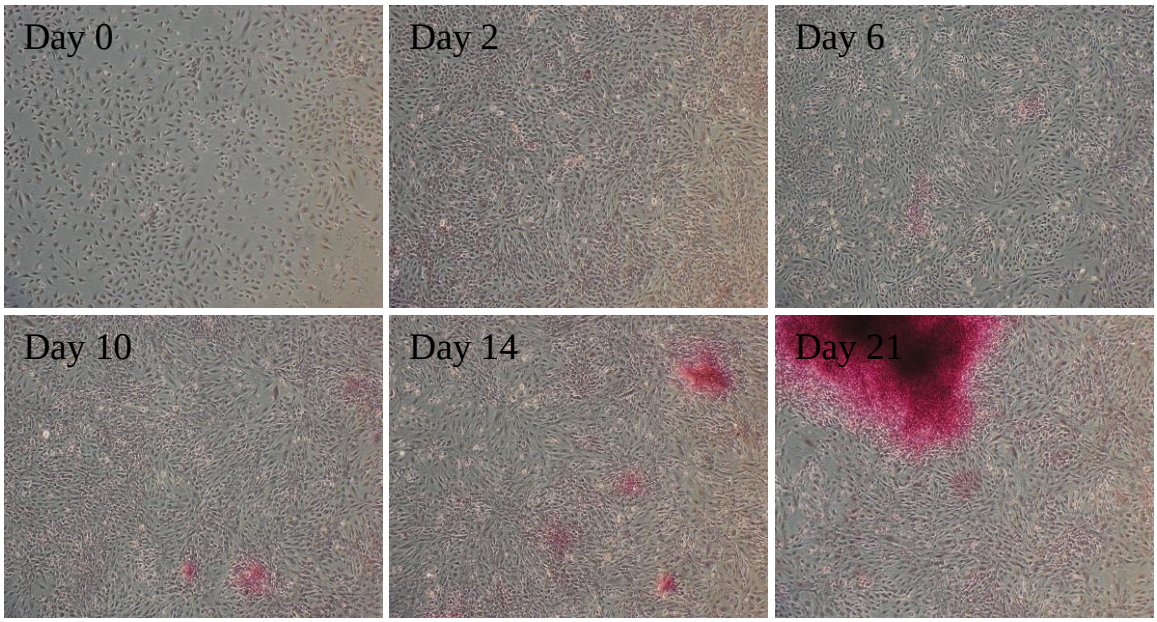

Fig. 10. Alizarin red stain for the visualization of the calcified extracellular matrix, Magn. ×40.

4.1.2. Expression of biological markers of chondrogenic differentiation

There was a statistical significant difference in the expression of Col2a1 during differentiation *in vitro* ($p = 0.003$). The expression of Col2a1 increased significantly on days 10 ($p = 0.02$) and 14 ($p = 0.03$; Fig. 11). The expression of Col10a1 also differed across the different days of measurements ($p < 0.0001$). Although not detectable at the beginning of differentiation, the expression of Col10a1 moderately increased on days 6 and 10, and became statistically significantly increased on days 14 ($p = 0.03$) and 21 ($p < 0.001$; Fig. 12).

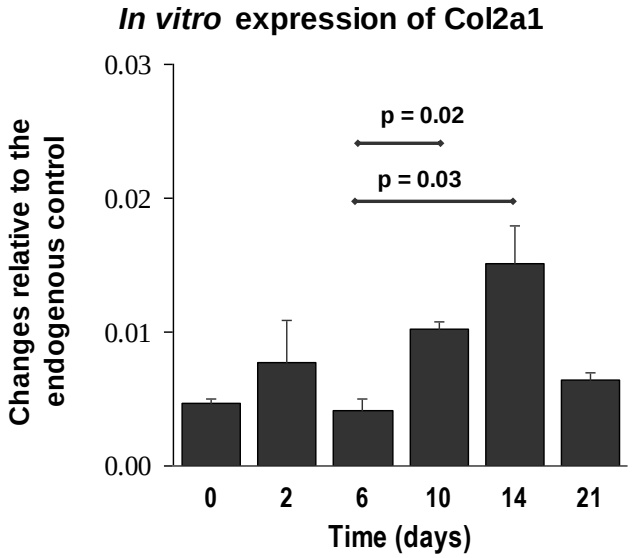

Fig. 11. Expression of Col2a1 early chondrogenic marker.

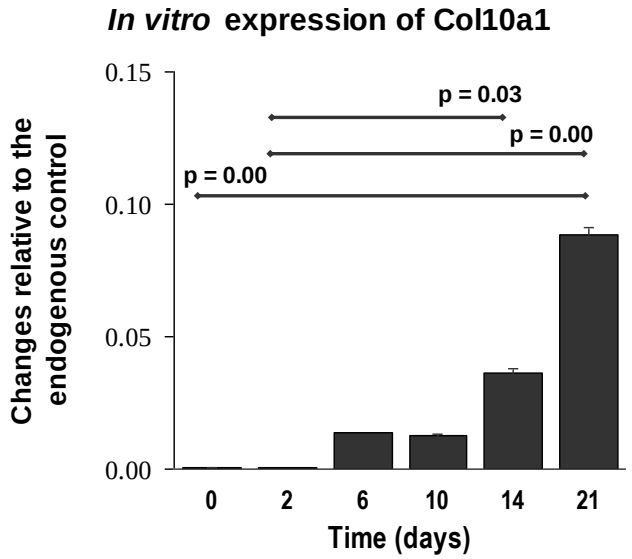

Fig. 12. Expression of Col10a1 late chondrogenic marker.

4.2. Expression pattern of Gpx1 *in vitro*

For Gpx1 investigated on the predetermined days, there was a statistically significant difference in its levels of expression during the 21 days ($N = 6$, $\chi 2(6) = 20.43$, $p < 0.01$).

Multiple comparisons identified a statistically significant increase relative to the endogenous control between the days 0 (18.3 ± 0.9) and 14 (117.6 ± 17.6, p = 0.03), 2 (17.6 ± 2.1) and 10 (78.2 ± 4.7, p = 0.02), and 2 (17.6 ± 2.1) and 14 (117.6 ± 17.6, p = 0.01; Fig. 13).

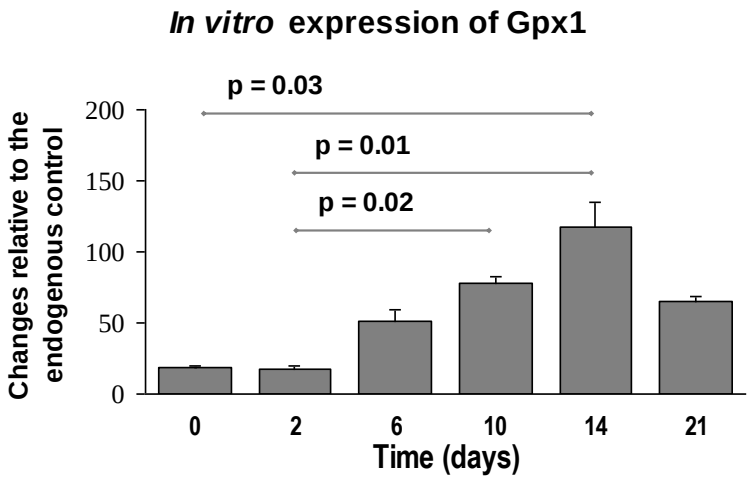

Fig. 13. Expression of Gpx1 during chondrogenic differentiation *in vitro* (from V. Koretsi et al., 2015).

4.3. Localization of Gpx1 expression at the spheno-occipital synchondrosis

The Cohen's Kappa for the inter-observer agreement was 0.797 ($p < 0.0001$), which indicates a substantial agreement. The Wilcoxon signed-rank test for repeatability between the time points of evaluation was not significant ($Z = -0.577$, $p = 0.56$). The immunoreactivity of Gpx1 was found to be statistically significantly different at the resting, proliferating, and hypertrophic zones of the spheno-occipital synchondrosis ($\chi2(2) = 15.200$, $p < 0.0001$; Fig. 14). The highest immunoreactivity was detected at the proliferating zones (4 ± 1), followed by the resting zone (3 ± 0.75). The hypertrophic zones demonstrated the lowest Gpx1 immunoreactivity (1.5 ± 1), which was statistical significant in comparison to the resting ($N = 8$, $Z = -2.64$, $p = 0.02$) and proliferating zones ($N = 8$, $Z = -2.59$, $p = 0.02$; Fig. 15).

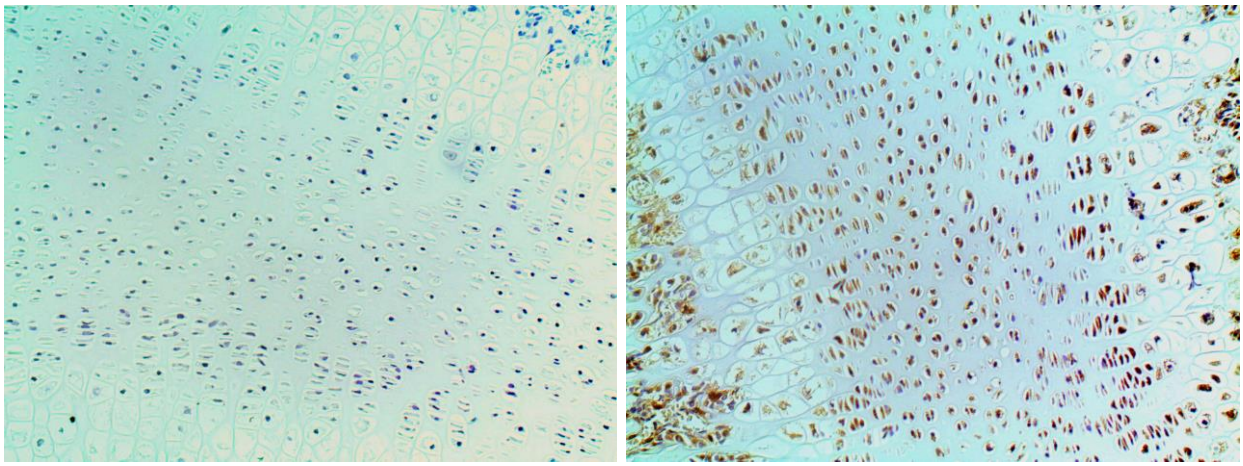

Fig. 14. Gpx1 immunoreactivity at the spheno-occipital synchondrosis of the rat, left: negative control, Magn. ×200 (adapted from V. Koretsi et al., 2015).

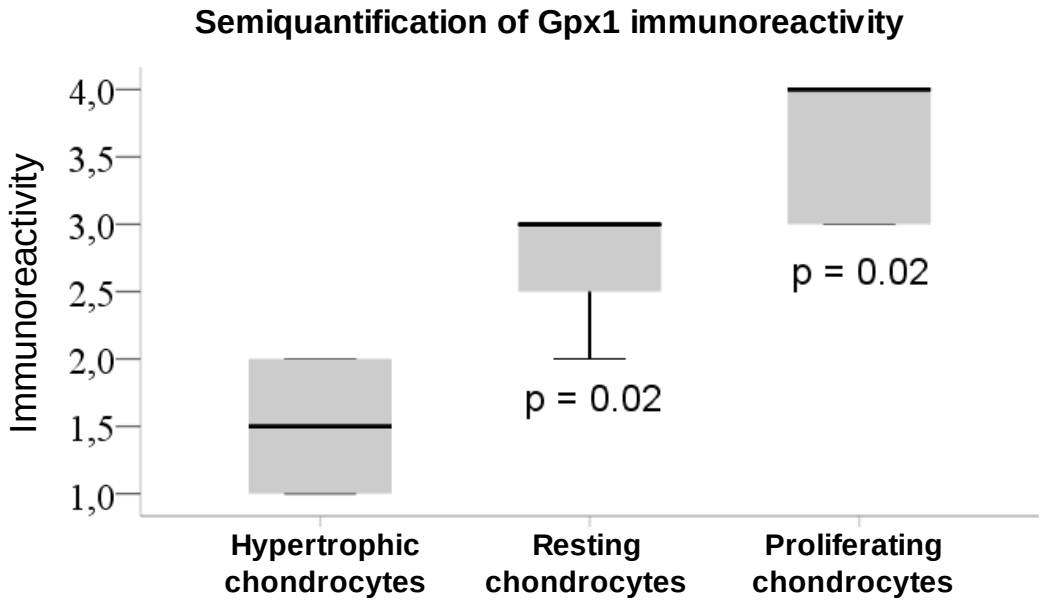

Fig. 15. Semiquantification of Gpx1 immunoreactivity at the spheno-occipital synchondrosis of the rat (adapted from V. Koretsi et al., 2015).

4.4. Apoptosis assay after exogenous exposure to H_2O_2

Results of the qRT-PCR for ensuring the manipulation of the Gpx1 expression are presented in Fig. 16. Furthermore, the expression of Gpx1 at the translational level was ensured with Western blot (Fig. 17). There was a statistically significant difference among groups as determined by Welch ANOVA ($F(2, 9.25) = 3718.6$, $p < 0.001$). The Games-Howell test showed that the apoptotic percentage of Gpx1-depleted chondrocytes was statistically significantly greater (66.1 ± 0.57%) compared to the control (17.7 ± 0.27%, $p < 0.001$) and cells overexpressing Gpx1 (10.9 ± 0.22%, $p < 0.001$). Furthermore, chondrocytes overexpressing Gpx1 had lower apoptotic rate (10.9 ± 0.22%) compared to control cells (17.7 ± 0.27%, $p < 0.001$; Fig. 18).

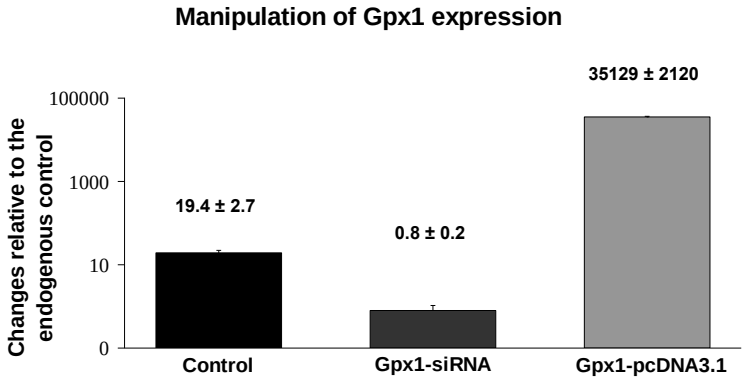

Fig. 16. Manipulation of Gpx1 expression measured with qRT-PCR. Gpx1-siRNA: Gpx1-depleted cells; Gpx1-pcDNA3.1: Gpx1-overexpressing cells (adapted from V. Koretsi et al., 2015).

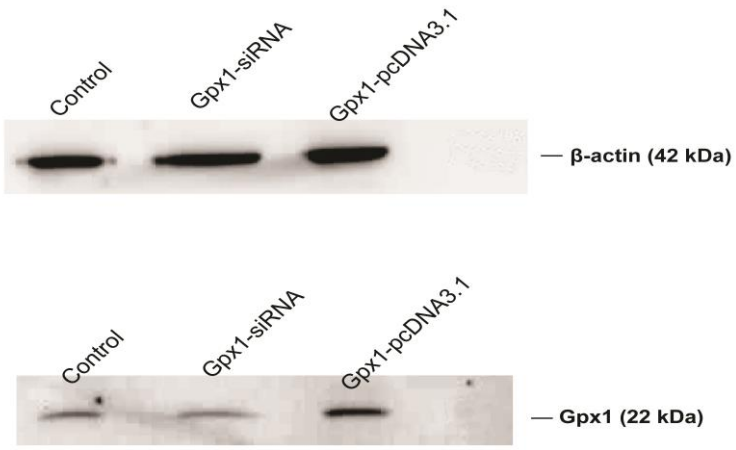

Fig. 17. Manipulation of Gpx1 expression measured with Western blot. Reference using as loading control β-actin (above) and ATDC5 cells under depletion or overexpression of Gpx1 (below). Gpx1-siRNA: Gpx1-depleted cells; Gpx1-pcDNA3.1: Gpx1-overexpressing cells.

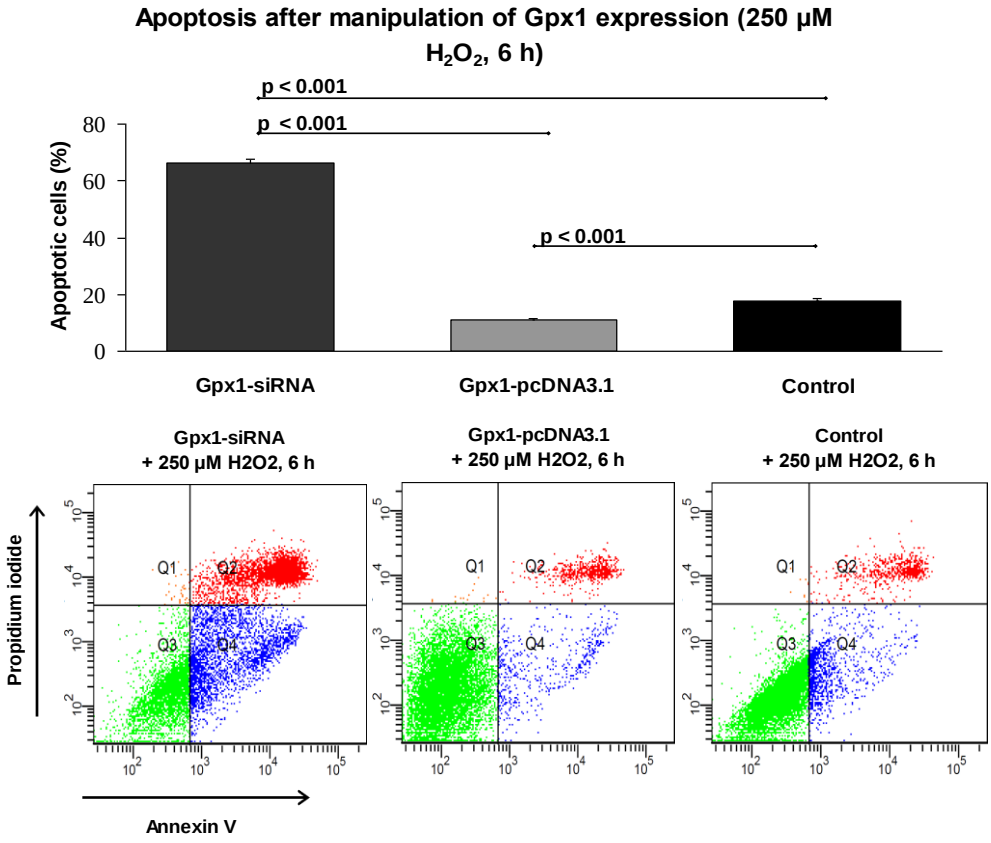

Fig. 18. Apoptotic cells after exposure to H_2O_2. Gpx1-siRNA: Gpx1-depleted cells; Gpx1-pcDNA3.1: Gpx1-overexpressing cells; Q1: dead cells; Q2: apoptotic cells; Q3: live cells; Q4: early apoptotic cells (adapted from V. Koretsi et al., 2015).

5. Discussion

Chondrogenesis represents the initial step of endochondral bone formation, the developmental mechanism of the synchondroses of the cranial base. Development and growth of the cranial base strongly influence facial shape (Cendekiawan et al., 2010) and are thus of interest in orthodontics. One of the most common antioxidant enzymes, Gpx1, has not been investigated in relation to chondrogenesis so far. Due to their function on reducing oxidative levels, antioxidant enzymes are generally presented as means to avoid oxidative damage in numerous pathological processes (Baynes, 1991; Kumar et al., 2008). However, oxidative stress, except for numerous pathological processes, also rises during developmental procedures (Thomas et al., 1997; El Mouatassim et al., 1999). From this point of view, antioxidants could play an equally relevant role on development because of their capability for neutralizing ROS.

In this study (Koretsi et al., 2015), the expression of Gpx1 gene was first monitored with qRT-PCR during chondrogenic differentiation *in vitro*, in an initial effort to observe and define its temporal expression pattern in chondrogenesis *in vitro*. It was observed that the expression of Gpx1 fluctuated during chondrogenic differentiation *in vitro*. On account of this, the next aim was to identify the extent of Gpx1 generation according to the differentiation stage of chondrocytes. For this purpose, Gpx1 was identified and localized through immunohistochemistry at the spheno-occipital synchondrosis of the cranial growth plate in rats. After discovering the different volumes of Gpx1-generation according to different stages of chondrogenic differentiation, the final objective was to determine the participation of Gpx1 in ROS scavenging as well as its impact on apoptosis in chondrocytes. The role of Gpx1 on ROS scavenging was flow cytometrically tested with an apoptotic assay in chondrogenic cells, whose Gpx1 levels were manipulated either with overexpression or knockdown *in vitro*.

5.1. Expression of Gpx1 during chondrogenic differentiation

The ATDC5 cell line used in this study is a well-accepted model for studying chondrogenic differentiation *in vitro*. In their review, Yao and Wang (2013) identified over 200 studies

utilizing the ATDC5 cell line to investigate bone formation. According to Altaf et al. (2006), the addition of vitamin C in the culture medium advances the differentiation of ATDC5 cells. In particular, an increase in biological markers of hypertrophic differentiation was observed within 7-10 days of administration of differentiation medium in experimental as compared to the control cultures. Therefore, it was concluded that hypertrophy occurs faster in ATDC5 cells growing in media additionally supplemented with vitamin C. In fact, that was not surprising, since vitamin C is widely recognised as a promoter of differentiation in other types of cells as well (Franceschi et al., 1994; Takahashi et al., 2003). Hence, it was decided to include vitamin C to medium composition in order to avoid a shift in medium and CO_2 concentration previously needed for inducing differentiation in ATDC5 cells (Shukunami et al., 1997).

The proposed mechanism of promoting differentiation through the addition of vitamin C in the medium is the formation of collagenous matrix, which in turn activates the ERK signalling pathway needed for differentiation (Temu et al., 2010). Except for vitamin C, the composition of the medium was as previously described (Shukunami et al., 1997). The differentiation of ATDC5 cells was verified with stains and expression of biological markers in this study. The colour intensity of the stains revealing proteoglycans and calcium in the matrix was increased during differentiation, while signs of cell aggregation were detected from day 10. On day 21, large cell condensations (cartilage nodules) were visible. These characteristics are consistent with cells undergoing chondrogenic differentiation (Shukunami et al., 1996; Shukunami et al., 1997). An emphasis must be put on the simultaneous increase in colour intensity for both stains, indicating that *in vitro* culture systems are difficult to be synchronised at the same differentiation stage (Pruszak et al., 2007). This practically means that proliferating and hypertrophic chondrocytes coexist in the same culture.

The aforementioned characteristic of the *in vitro* culture systems has an influence on the expression of chondrogenic biological markers too. The expression of Col2a1 reached a peak on day 14, while Col10a1 on day 21. These findings are similar to those of Altaf et al. (2006), who utilised the same medium. However, the expression of Col10a1 was hardly detectable at the beginning and became visible from day 6 onwards, possibly indicating that hypertrophy in some cells began from that timepoint.

Hence, it could be assumed that the increase in Gpx1 expression between the days 6 and 14 coincided the hypertrophic status of some cells in the culture. However, this could serve only

as an estimate and not as a conclusion. On the contrary, the reliably drawn conclusion is that Gpx1 expression is not of constitutive nature during chondrogenic differentiation.

5.2. Hypertrophic chondrocytes have the lowest Gpx1-immunoreactivity

As opposed to the aforementioned limitation of *in vitro* conditions, *ex vivo* experiments can provide with a more realistic point of view. Therefore, the expression of Gpx1 was identified and localized at the spheno-occipital synchondrosis of rats. The potentiality of localizing the expression of Gpx1 at a specific differentiation stage increases with immunohistochemistry because the clearly distinct arrangement of chondrocytes in regard to their differentiation stage is preserved in the samples under investigation.

Moreover, the frequently occurring variation in cellular transcriptome and proteome must be considered as a potential threat to the interpretation of gene expression data. Post-transcriptional processing, mRNA degradation, and post-translational regulation strongly affect the cellular concentrations of proteins. The squared Pearson correlation coefficient between protein levels and their corresponding mRNA abundances amounted approximately 0.40 for both bacteria and eukaryotes. This finding shows that 60% of the variation in protein levels can not be explained by knowing mRNA concentrations (Vogel and Marcotte, 2012). In addition, a modest correlation between mRNA and protein levels was reported for mouse (Ghazalpour et al., 2011). These data suggest that the concordance between transcriptome and proteome must not be taken for granted. Provided that cell function is dictated by proteins, immunohistochemistry is more reliable than the identification of genes, since it reveals the expression of proteins.

The semiquantitative results of the Gpx1 protein expression at the spheno-occipital synchondrosis of the rat show that proliferative chondrocytes have the highest Gpx1 immunoreactivity, followed by resting chondrocytes. The lowest levels of Gpx1 immunoreactivity were identified in hypertrophic chondrocytes. Similar to the present findings, lower activity of SOD, Gpx4, and catalase has been reported for hypertrophic chondrocytes compared to other stages of chondrogenic differentiation (Matsumoto et al., 1991; Fragonas et al., 1998). The lower expression of antioxidant enzymes leads to higher levels of ROS in hypertrophic compared to proliferating or resting chondrocytes, as

previously reported (Morita et al., 2007). NADPH oxidases 1 and 2 contribute to ROS levels during hypertrophy, since they were highly expressed in prehypertrophic and hypertrophic chondrocytes (Kim et al., 2010). Especially the depletion of NADPH oxidase 2 resulted in abnormal chondrogenic differentiation (Kim et al., 2010). Finally, ROS elevation inhibits proliferation and initiates hypertrophy of chondrocytes (Morita et al., 2007). This could match the present results, as proliferating zones demonstrated the highest Gpx1 immunoreactivity and hypertrophic zones the lowest one.

However, immunohistochemical detection is accompanied by specific limitations. It is considered a semiquantitative method based on observer's visual scoring and, as such, is subjective (Taylor and Levenson, 2006), which in turn leads to inter- and intra-observer variability. Nevertheless, although computer-assisted quantification works faster, it is not always associated with better results (Matos et al., 2006; Ong et al., 2010). In the present study, an effort was made to account for inter- and intra-observer variability. The inter-observer agreement was found to be substantial and the intra-observer variability was not statistically significant.

5.3. Gpx1 plays a vital role on H_2O_2-induced apoptosis in chondrocytes

After determining the distribution pattern of Gpx1 protein expression at the spheno-occipital synchondrosis, the effect of Gpx1 on chondrocytes was investigated *in vitro*. Provided that Gpx1 catalyses the reaction $2GSH + H_2O_2 \rightarrow GSSG + 2H_2O$ (Kulinsky and Kolesnichenko, 2009), ATDC5 cells were treated with 250 μM H_2O_2. To define the role of Gpx1 on H_2O_2 scavenging, three groups were established: Gpx1-overexpressing cells, Gpx1-knockdown cells, and control cells. The apoptotic percentage of cells was then flow-cytometrically measured with FITC-labelled Annexin V in conjunction with PI dye.

Annexin V as a means to detect apoptosis was first described by Koopman et al. (1994). It demonstrates high affinity to membrane phospholipid phosphatidylserine (Andree et al., 1990), which is translocated from the internal to the external cellular environment (Fadok et al., 1992) in apoptotic cells. The PI dye is simultaneously used for discriminating between dead and apoptotic cells (van Engeland et al., 1998). This procedure has certain advantages, one of the most important being the detection of the early stages of apoptosis through changes

of the cell surface. DNA-associated changes occur rather late in apoptosis and assays detecting those changes are thus less precise than Annexin V (Zhang et al., 1997). Further, fluorescence of the samples was quantified with flow cytometry. Flow cytometry is an accurate method for quantifying fluorescence and presents advantages over fluorescence microscopy, namely flow cytometry is more objective, reproducible, and sensitive (Bolaños et al., 1988; Torous et al., 2003; Muratori et al., 2008).

Results obtained with the aforementioned method revealed that Gpx1 is necessary for chondrocytes, since Gpx1-depleted chondrocytes essentially underwent apoptosis at the highest percentage under H_2O_2 exposure. On the contrary, Gpx1-overexpressing chondrocytes had the lowest apoptotic percentage. These results are suggestive of the vital role of Gpx1 on H_2O_2 scavenging and, consequently, H_2O_2-induced apoptosis in chondrocytes.

However, Gpx1 is not the only one source of H_2O_2 degradation. Catalase also belongs to the antioxidant enzymatic defence system and reduces H_2O_2 according to the following reaction: $2H_2O_2 \rightarrow 2H_2O + O_2$ (Kalyanaraman, 2013). Therefore, the role of catalase on H_2O_2-induced apoptosis needs elucidation in chondrocytes, although catalase was shown to be inactivated (Lardinois et al., 1996; Baud et al., 2004) in the presence of high concentrations of H_2O_2. In addition to this, catalase seemed to be dependent on Gpx1 activity to prevent its inactivation at high concentrations of H_2O_2 (Baud et al., 2004).

6. Summary

Orthodontics deals with the correction of skeletal anomalies of the face occurring in the form of jaw discrepancies. There is an abundance of findings in the literature that the development and growth of the cranial base influence facial shape and jaw discrepancies. Cranial base develops by the mechanism of endochondral ossification taking place at its midline axis, where all the synchondroses are located. Chondrogenesis is the initial and indispensable part of endochondral bone formation. In the light of evidence underlying the need of reactive oxygen species in the regulation of chondrogenesis, this study aimed to investigate the ubiquitously present antioxidant enzyme Gpx1 and its contribution to redox regulation in chondrogenesis.

Provided that the levels of oxidative stress were previously found to fluctuate according to the differentiation stage of chondrocytes, the gene expression of Gpx1 was measured with quantitative RT-PCR during chondrogenic differentiation. For this purpose, the chondrogenic cell line ATDC5 was utilized and cultured for 21 days. The time points of measurements were on days 0, 2, 6, 10, 14, and 21. The chondrogenic differentiation of the utilized cell line was determined with the stains Alcian blue and Alizarin red, and with the gene expression of chondrogenic biological markers Col2a1 and Col10a1. The present results suggest that the expression of Gpx1 is not of constitutive nature during chondrogenic differentiation.

Taking this as a starting point, the next step was to quantitatively assess the distribution pattern of Gpx1 at the different differentiation stages of chondrogenesis. To examine this, the spheno-occipital synchondrosis from eight newborn male Wistar rats was isolated and samples were processed for formaldehyde-fixed paraffin-embedded immunohistochemistry. Photographs of the immunostained sections were analysed by two independent observers and a five-grade semiquantitative scale was used to assess Gpx1 immunoreactivity at the synchondrosis. The present findings show that Gpx1 is expressed the most at the proliferative differentiation stage and the lowest at the hypertrophic differentiation stage. Existing literature reports that an increase in oxidative levels is needed for inhibition of proliferation and initiation of hypertrophy. Further, chondrocytes at the hypertrophic stage have the highest levels of ROS compared to other differentiation stages. In this context, the present results implied that Gpx1 is involved in redox regulation in chondrogenesis.

To pursue this further, the expression of Gpx1 was manipulated in ATDC5 chondrogenic cells and cells were then exposed to exogenous H_2O_2. The manipulation of Gpx1 expression included overexpression and silencing. A control group was also included. The apoptotic percentage of cells was measured flow cytometrically with FITC-labelled Annexin V in conjunction with PI dye. The highest apoptotic percentage was observed in Gpx1-depleted chondrocytes, followed by the control group. The lowest apoptotic percentage was presented in Gpx1-overexpressing cells. These results indicate that Gpx1 possesses an active role on the cellular enzymatic antioxidant system of chondrocytes and can regulate the cellular redox state by H_2O_2 scavenging. Furthermore, its presence in chondrocytes can prevent H_2O_2-induced apoptosis.

The contribution of cranial base growth to craniofacial morphology continues until adulthood, since spheno-occipital synchondrosis is the last of the synchondroses to ossify and is active until then. This study localizes the expression of Gpx1 at the spheno-occipital synchondrosis and documents the role of Gpx1 as a redox regulator in chondrocytes.

7. Zusammenfassung

Die Kieferorthopädie befasst sich mit der Prävention, Diagnostik und Therapie von Skelettanomalien des Gesichts, welche in Form von Kieferfehlstellungen auftreten. Eine Fülle von Forschungsergebnissen besagt, dass die Entwicklung und das Wachstum der Schädelbasis die Gesichtsform und damit Kieferfehlstellungen beeinflussen. Die Schädelbasis entwickelt durch den Mechanismus der enchondralen Ossifikation, die an ihrer mittleren Achse stattfindet, wo sich alle Synchondrosen befinden. Chondrogenese ist der erste und unverzichtbare Bestandteil der enchondralen Ossifikation. Angesichts der Beweise für die Notwendigkeit der reaktiven Sauerstoffspezies in der Regulation der Chondrogenese, sollte diese Studie das allgegenwärtig vorhandene antioxidative Enzym Gpx1 und dessen Beitrag zur Redoxregulation während der Chondrogenese untersuchen.

Vorausgesetzt, dass das Niveau von oxidativem Stress entsprechend dem Differenzierungsstadium der Chondrozyten schwankt, wurde die Genexpression von Gpx1 mit quantitativer RT-PCR während der chondrogenen Differenzierung gemessen. Zu diesem Zweck wurde die chondrogene Zelllinie ATDC5 verwendet und für 21 Tage kultiviert. Die Messzeitpunkte wurden an den Tagen 0, 2, 6, 10, 14 und 21 ausgewählt. Die chondrogene Differenzierung der verwendeten Zelllinie wurde mit den Färbungen Alcian-Blau und Alizarin-Rot bestimmt und mit der Genexpression von chondrogenen biologischen Markern Col2a1 und Col10a1 verglichen. Die vorliegenden Ergebnisse deuten darauf hin, dass die Expression von Gpx1 nicht von konstitutiver Natur während der chondrogenen Differenzierung ist.

Auf dieser Basis wurde das Verteilungsmuster von Gpx1 in den verschiedenen Differenzierungsstadien der Chondrogenese näher untersucht. Die Synchondrosis spheno-occipitalis wurde aus acht neugeborenen männlichen Wistar-Ratten isoliert. Die Proben wurden für Formaldehyd-fixierte und Paraffin-eingebettete Immunhistochemie weiterverarbeitet. Eine fünfstufige semiquantitative Skala wurde verwendet, um die Gpx1-Immunreaktivität bei der Synchondrosis spheno-occipitalis zu bestimmen. Fotografien der immungefärbten Abschnitte wurden von zwei unabhängigen Beobachtern bewertet. Die vorliegenden Ergebnisse zeigen, dass Gpx1 am meisten bei den proliferativen Chondrozyten und am wenigsten bei den hypertrophen Chondrozyten exprimiert wird. Existierende Literatur berichtet, dass eine Erhöhung des oxidativen Niveaus für die Hemmung der Proliferation und

die Einleitung der Hypertrophie nötig ist. Weiterhin weisen Chondrozyten im hypertrophen Stadium das höchste Niveau von ROS im Vergleich zu anderen Differenzierungsstadien auf. In diesem Zusammenhang implizierten die vorliegenden Ergebnisse, dass Gpx1 an der Redoxregulation während der Chondrogenese beteiligt ist.

Um dies weiter zu verfolgen, wurde die Expression von Gpx1 in ATDC5 chondrogenen Zellen manipuliert und Zellen wurden dann exogenem H_2O_2 ausgesetzt. Die Manipulation der Gpx1-Expression enthielt Überexpression und Silencing. Eine Kontrollgruppe wurde ebenfalls eingeschlossen. Der apoptotische Prozentsatz der Zellen wurde durchflusszytometrisch mit FITC-Annexin V und -Propidiumiodid-Färbung gemessen. Der höchste apoptotische Prozentsatz wurde in Gpx1-ausgeschalteten Chondrozyten beobachtet, gefolgt von der Kontrollgruppe. Der niedrigste apoptotische Prozentsatz wurde in Gpx1-überexprimierenden Zellen präsentiert. Diese Ergebnisse zeigen, dass Gpx1 eine aktive Rolle im zellulären enzymatischen Antioxidationssystem der Chondrozyten besitzt und den zellulären Redoxzustand durch H_2O_2-Abbau regeln kann. Darüber hinaus kann seine Präsenz in Chondrozyten H_2O_2-induzierte Apoptose verhindern.

Der Einfluss des Schädelbasiswachstums auf die kraniofaziale Morphologie bleibt bis ins frühe Erwachsenenalter bestehen, da die Synchondrosis spheno-occipitalis bis dahin aktiv bleibt. Diese Studie lokalisiert die Expression von Gpx1 an der Synchondrosis spheno-occipitalis und dokumentiert die Rolle von Gpx1 als Redox-Regler in Chondrozyten.

8. References

Adams, C. S., Shapiro, I. M., 2002. The fate of the terminally differentiated chondrocyte: evidence for microenvironmental regulation of chondrocyte apoptosis. Crit. Rev. Oral Biol. Med. 13, 465-473.

Ahmed, Y. A., Tatarczuch, L., Pagel, C. N., Davies, H. M., Mirams, M., Mackie, E. J., 2007. Physiological death of hypertrophic chondrocytes. Osteoarthr. Cartil. 15, 575-586.

Aitken, R. J., Roman, S. D., 2008. Antioxidant systems and oxidative stress in the testes. Oxid. Med. Cell Longev. 1, 15-24.

Akiyama, H., Lyons, J. P., Mori-Akiyama, Y., Yang, X., Zhang, R., Zhang, Z., Deng, J. M., Taketo, M. M., Nakamura, T., Behringer, R. R., McCrea, P. D., de Crombrugghe, B., 2004. Interactions between Sox9 and beta-catenin control chondrocyte differentiation. Genes Dev. 18, 1072-1087.

Altaf, F. M., Hering, T. M., Kazmi, N. H., Yoo, J. U., Johnstone, B., 2006. Ascorbate-enhanced chondrogenesis of ATDC5 cells. Eur. Cell Mater. 12, 64-69.

Anagastopolou, S., Karamaliki, D. D., Spyropoulos, M. N., 1988. Observations on the growth and orientation of the anterior cranial base in the human foetus. Eur. J. Orthod. 10, 143-148.

Anderson, D. R., 1964. The ultrastructure of elastic and hyaline cartilage of the rat. Am. J. Anat. 114, 403-434.

Anderson, D., Popovich, F., 1983. Relation of cranial base flexure to cranial form and mandibular position. Am. J. Phys. Anthropol. 61, 181-187.

Anderson, H. C., Sipe, J. B., Hessle, L., Dhanyamraju, R., Atti, E., Camacho, N. P., Millan, J. L., 2004. Impaired calcification around matrix vesicles of growth plate and bone in alkaline phosphatase-deficient mice. Am. J. Pathol. 164, 841-847.

Andrade, A. C., Nilsson, O., Barnes, K. M., Baron, J., 2007. Wnt gene expression in the post-natal growth plate: regulation with chondrocyte differentiation. Bone 40, 1361-1369.

Andree, H. A., Reutelingsperger, C. P., Hauptmann, R., Hemker, H. C., Hermens, W. T., Willems, G. M., 1990. Binding of vascular anticoagulant alpha (VAC alpha) to planar phospholipid bilayers. J. Biol. Chem. 265, 4923-4928.

Arnold, R.S., Shi, J., Murad, E., Whalen, A. M., Sun, C. Q., Polavarapu, R., Parthasarathy, S., Petros, J. A., Lambeth, J. D., 2001. Hydrogen peroxide mediates the cell growth and transformation caused by the mitogenic oxidase Nox1. Proc. Natl. Acad. Sci. USA 98, 5550-5555.

Atsumi, T., Miwa, Y., Kimata, K., Ikawa, Y., 1990. A chondrogenic cell line derived from a differentiating culture of AT805 teratocarcinoma cells. Cell Diff. Dev. 30, 109-116.

Bacon, W., Eiller, V., Hildwein, M., Dubois, G., 1992. The cranial base in subjects with dental and skeletal Class II. Eur. J. Orthod. 14, 224-228.

Baud, O., Greene, A. E., Li, J., Wang, H., Volpe, J. J., Rosenberg, P. A., 2004. Glutathione peroxidase-catalase cooperativity is required for resistance to hydrogen peroxide by mature rat oligodendrocytes. J. Neurosci. 24, 1531-1540.

Baynes, J. W., 1991. Role of oxidative stress in development of complications in diabetes. Diabetes 40, 405-412.

Bjork, A., 1955. Cranial base development. Am. J. Orthod. 41, 198-225.

Bolaños, B., Bodón, Q., Jiménez, T., García-Mayol, D., Lavergne, J. A., Díaz, A. M., 1988. Analysis by fluorescence microscopy and flow cytometry of monoclonal antibodies produced against cell surface antigens. P. R. Health Sci. J. 7, 35-38.

Cai, H., 2005. Hydrogen peroxide regulation of endothelial function: origins, mechanisms, and consequences. Cardiovasc. Res. 68, 26-36.

Cendekiawan, T., Wong, R. W., Rabie, A. B. M., 2010. Relationships between cranial base synchondroses and craniofacial development: a review. Open Anat. J. 2, 67-75.

Chang, H. P., Chou, T. M., Hsieh, S. H., Tseng, Y. C., 2005. Cranial-base morphology in children with class III malocclusion. Kaohsiung J. Med. Sci. 21, 159-165.

Chang, T. S., Cho, C. S., Park, S., Yu, S., Kang, S. W., Rhee, S. G., 2004. Peroxiredoxin III, a mitochondrion-specific peroxidase, regulates apoptotic signaling by mitochondria. J. Biol. Chem. 279, 41975-41984.

Chen, M., Zhu, M., Awad, H., Li, T. F., Sheu, T. J., Boyce, B. F., Chen, D., O'Keefe, R. J., 2008. Inhibition of beta-catenin signaling causes defects in postnatal cartilage development. J. Cell Sci. 121, 1455-1465.

Chen, Q., Espey, M. G., Krishna, M. C., Mitchell, J. B., Corpe, C. P., Buettner, G. R., Shacter, E., Levine, M., 2005. Pharmacologic ascorbic acid concentrations selectively kill cancer cells: action as a pro-drug to deliver hydrogen peroxide to tissues. Proc. Natl. Acad. Sci. USA 102, 13604-13609.

Choi, M. H., Lee, I. K., Kim, G. W., Kim, B. U., Han, Y. H., Yu, D. Y., Park, H. S., Kim, K. Y., Lee, J. S., Choi, C., Bae, Y. S., Lee, B. I., Rhee, S. G., Kang, S. W., 2005. Regulation of PDGF signalling and vascular remodelling by peroxiredoxin II. Nature 435, 347-353.

Chuang, C. Y., Lord, M. S., Melrose, J., Rees, M. D., Knox, S. M., Freeman, C., Iozzo, R. V., Whitelock, J. M., 2010. Heparan sulfate-dependent signaling of fibroblast growth factor 18 by chondrocyte-derived perlecan. Biochemistry 49, 5524-5532.

Cobourne, M. T., DiBiase, A. T., 2010. Handbook of orthodontics, Mosby, Edinburgh.

Colnot, C. I., Helms, J. A., 2001. A molecular analysis of matrix remodeling and angiogenesis during long bone development. Mech. Dev. 100, 245-250.

Colnot, C., Lu, C., Hu, D., Helms, J. A., 2004. Distinguishing the contributions of the perichondrium, cartilage, and vascular endothelium to skeletal development. Dev. Biol. 269, 55-69.

Couly, G. F., Coltey, P. M., Le Douarin, N. M., 1993. The triple origin of skull in higher vertebrates. Develop. 117, 409-429.

Covarrubias, L., Hernández-García, D., Schnabel, D., Salas-Vidal, E., Castro-Obregón, S., 2008. Function of reactive oxygen species during animal development: passive or active? Dev. Biol. 320, 1-11.

Davies, K. J., 2000. Oxidative stress, antioxidant defenses, and damage removal, repair, and replacement systems. IUBMB Life 50, 279-289.

Deckers, M. M., Van Beek, E. R., Van Der Pluijm, G., Wetterwald, A., Van Der Wee-Pals, L., Cecchini, M. G., Papapoulos, S. E., Lowik, C. W., 2002. Dissociation of angiogenesis and osteoclastogenesis during endochondral bone formation in neonatal mice. J. Bone Min. Res. 17, 998-1007.

Dhopatkar, A., Bhatia, S., Rock, P., 2002. An investigation into the relationship between the cranial base angle and malocclusion. Angle Orthod. 72, 456-463.

Dibbets, J. M. H., 1996. Morphological associations between the Angle classes. Eur. J. Orthod. 18, 111-118.

Diewert, V. M., 1985. Development of human craniofacial morphology during the late embryonic and early fetal periods. Am. J. Orthod. 88, 64-76.

Dröge, W., 2002. Free radicals in the physiological control of cell function. Physiol. Rev. 82, 47-95.

El Mouatassim, S., Guérin, P., Ménézo, Y., 1999. Expression of genes encoding antioxidant enzymes in human and mouse oocytes during the final stages of maturation. Mol. Hum. Reprod. 5, 720-725.

Enlow, D. H., 1968. The human face, Hoeber Medical Division, New York.

Enlow, D. H., 1990. Facial growth, Saunders, Philadelphia.

Enlow, D. H., Hans, M. G., 1996. Essentials of facial growth, Saunders, Philadelphia.

Enomoto, H., Enomoto-Iwamoto, M., Iwamoto, M., Nomura, S., Himeno, M., Kitamura, Y., Kishimoto, T., Komori, T., 2000. Cbfa1 is a positive regulatory factor in chondrocyte maturation. J. Biol. Chem. 275, 8695-8702.

Enomoto-Iwamoto, M., Kitagaki, J., Koyama, E., Tamamura, Y., Wu, C., Kanatani, N., Koike, T., Okada, H., Komori, T., Yoneda, T., Church, V., Francis-West, P. H., Kurisu, K., Nohno, T., Pacifici, M., Iwamoto, M., 2002. The Wnt antagonist Frzb-1 regulates chondrocyte maturation and long bone development during limb skeletogenesis. Dev. Biol. 251, 142-156.

Fadok, V. A., Voelker, D. R., Campbell, P. A., Cohen, J. J., Bratton, D. L., Henson, P. M., 1992. Exposure of phosphatidylserine on the surface of apoptotic lymphocytes triggers specific recognition and removal by macrophages. J. Immunol. 148, 2207-2216.

Fedde, K. N., Blair, L., Silverstein, J., Coburn, S. P., Ryan, L. M., Weinstein, R. S., Waymire, K., Narisawa, S., Millan, J. L., MacGregor, G. R., Whyte, M. P., 1999. Alkaline phosphatase knock-out mice recapitulate the metabolic and skeletal defects of infantile hypophosphatasia. J. Bone Min. Res. 14, 2015-2026.

Flohé, L., Brigelius-Flohé, R., 2012. Selenoproteins of the Glutathione Peroxidase Family. In: Hatfield, D. L., Berry, M. J., Gladyshev, V. N. (Ed.). Selenium. Springer, New York, 167-

180.

Forman, H. J., Fukuto, J. M., Torres, M., 2004. Redox signaling: thiol chemistry defines which reactive oxygen and nitrogen species can act as second messengers. Am. J. Physiol. Cell Physiol. 287, C246-256.

Fragonas, E., Pollesello, P., Mlinárik, V., Toffanin, R., Grando, C., Godeas, C., Vittur, F., 1998. Sensitivity of chondrocytes of growing cartilage to reactive oxygen species. Biochim. Biophys. Acta 1425, 103-111.

Franceschi, R. T., Iyer, B. S., Cui, Y., 1994. Effects of ascorbic acid on collagen matrix formation and osteoblast differentiation in murine MC3T3-E1 cells. J. Bone Min. Res. 9, 843-854.

Franchi, L., Baccetti, T., Stahl, F., McNamara Jr, J. A., 2007. Thin-plate spline analysis of craniofacial growth in Class I and Class II subjects. Angle Orthod. 77, 595-601.

Gartland, A., Mason-Savas, A., Yang, M., MacKay, C. A., Birnbaum, M. J., Odgren, P. R., 2009. Septoclast deficiency accompanies postnatal growth plate chondrodysplasia in the toothless (tl) osteopetrotic, colony-stimulating factor-1 (CSF-1)-deficient rat and is partially responsive to CSF-1 injections. Am. J. Pathol. 175, 2668-2675.

Gentili, C., Cancedda, R., 2009. Cartilage and bone extracellular matrix. Curr. Pharm. Des. 15, 1334-1348.

Ghazalpour, A., Bennett, B., Petyuk, V. A., Orozco, L., Hagopian, R., Mungrue, I. N., Farber, C. R., Sinsheimer, J., Kang, H. M., Furlotte, N., Park, C. C., Wen, P. Z., Brewer, H., Weitz, K., Camp, D. G. 2nd, Pan, C., Yordanova, R., Neuhaus, I., Tilford, C., Siemers, N., Gargalovic, P., Eskin, E., Kirchgessner, T., Smith, D. J., Smith, R. D., Lusis, A. J., 2011. Comparative analysis of proteome and transcriptome variation in mouse. PLoS Genet. 7, e1001393.

Giles, W. B., Philips, C. L., Joondeph, D. R., 1981. Growth in the basicranial synchondroses of adolescent Macaca mullata. Anat. Rec. 19, 259-266.

Goldring, M. B., Tsuchimochi, K., Ijiri, K., 2006. The control of chondrogenesis. J. Cell Biochem. 97, 33-44.

Grassel, S., Ahmed, N., 2007. Influence of cellular microenvironment and paracrine signals on chondrogenic differentiation. Front. Biosci. 12, 4946-4956.

Heinegard, D., 2009. Proteoglycans and more – from molecules to biology. Int. J. Exp. Pathol. 90, 575-586.

Henrikson, R. C., Kaye, G. I., Mazurkiewicz, J. E., 1997. Histology, Williams & Wilkins, Baltimore.

Hofer, H., 1960. Studien zum Problem des Gestaltwandels des Schädels der Säugetiere, insbesondere der Primaten: I. Die medianen Krümmungen des Schädels und ihre Erfassung nach der Methode von Landzert. Z. Morphol. Anthropol. 50, 299-316.

Hofer, H., Spatz, W., 1963. Studien zum Problem des Gestaltwandels des Schädels der Säugetiere, insbesondere der Primaten: II. Über die Kyphosen fetaler und neonater Primatenschädel. Z. Morphol. Anthropol. 53, 29-52.

Hopkin, G. B., Houston, W. J. B., James, G. A., 1968. The cranial base as an etiological factor in malocclusion. Angle Orthod. 38, 250-255.

Hoyte, D. A., 1991. The cranial base in normal and abnormal skull growth. Neurosurg. Clin. N. Am. 2, 515-537.

Huang, W., Zhou, X., Lefebvre, V., de Crombrugghe, B., 2000. Phosphorylation of SOX9 by cyclic AMP-dependent protein kinase A enhances SOX9's ability to transactivate a Col2a1 chondrocyte-specific enhancer. Mol. Cell Biol. 20, 4149-4158.

Hurd, T. R., DeGennaro, M., Lehmann, R., 2012. Redox regulation of cell migration and adhesion. Trends Cell Biol. 22, 107-115.

Inada, M., Wang, Y., Byrne, M. H., Rahman, M. U., Miyaura, C., Lopez-Otin, C., Krane, S. M., 2004. Critical roles for collagenase-3 (Mmp13) in development of growth plate cartilage and in endochondral ossification. Proc. Natl. Acad. Sci. USA 101, 17192-17197.

Kalyanaraman, B., 2013. Teaching the basics of redox biology to medical and graduate students: Oxidants, antioxidants and disease mechanisms. Redox Biol. 1, 244-257.

Kerr, W. J. S., Hirst, D., 1987. Craniofacial characteristics of subjects with normal and postnormal occlusions–a longitudinal study. Am. J. Orthod. Dentofac. Orthop. 92, 207-212.

Kim, K. S., Choi, H. W., Yoon, H. E., Kim, I. Y., 2010. Reactive oxygen species generated by NADPH oxidase 2 and 4 are required for chondrogenic differentiation. J. Biol. Chem. 285, 40294-40302.

Kirsch, T., 2006. Determinants of pathological mineralization. Curr. Opin. Rheumatol. 18, 174-180.

Kirsch, T., Nah, H. D., Shapiro, I. M., Pacifici, M., 1997. Regulated production of mineralization-competent matrix vesicles in hypertrophic chondrocytes. J. Cell Biol. 137, 1149-1160.

Kishimoto, K., Kitazawa, R., Kurosaka, M., Maeda, S., Kitazawa, S., 2006. Expression profile of genes related to osteoclastogenesis in mouse growth plate and articular cartilage. Histochem. Cell Biol. 125, 593-602.

Kjaer, I., 1990. Ossification of the human basicranium. J. Craniofac. Genet. Dev. Biol. 10, 29-38.

Knußmann, R., 1988. Anthropologie. Handbuch der vergleichenden Biologie des Menschen. Bd. 1/I, Fischer, Stuttgart.

Kobayashi, T., Soegiarto, D. W., Yang, Y., Lanske, B., Schipani, E., McMahon, A. P., Kronenberg, H. M., 2005. Indian hedgehog stimulates periarticular chondrocyte differentiation to regulate growth plate length independently of PTHrP. J. Clin. Invest. 115, 1734-1742.

Komori, T., 2005. Regulation of skeletal development by the Runx family of transcription factors. J. Cell Biochem. 95, 445-453.

Koopman, G., Reutelingsperger, C. P., Kuijten, G. A., Keehnen, R. M., Pals, S. T., Van Oers, M. H., 1994. Annexin V for flow cytometric detection of phosphatidylserine expression on B cells undergoing apoptosis. Blood 84, 1415-1420.

Koretsi, V., Kirschneck, C., Proff, P., Römer, P., 2015. Expression of glutathione peroxidase 1 in the spheno-occipital synchondrosis and its role in ROS-induced apoptosis. Eur. J. Orthod. 37, 308-313.

Koyama, E., Young, B., Nagayama, M., Shibukawa, Y., Enomoto-Iwamoto, M., Iwamoto, M., Maeda, Y., Lanske, B., Song, B., Serra, R., Pacifici M., 2007. Conditional Kif3a ablation causes abnormal hedgehog signaling topography, growth plate dysfunction, and excessive bone and cartilage formation during mouse skeletogenesis. Develop. 134, 2159-2169.

Kulinsky, V. I., Kolesnichenko, L. S., 2009. The glutathione system. I. Synthesis, transport, glutathione transferases, glutathione peroxidases. Biochem. (Mosc.) Suppl. Ser. B 3, 129-144.

Kumar, B., Koul, S., Khandrika, L., Meacham, R. B., Koul, H. K., 2008. Oxidative stress is inherent in prostate cancer cells and is required for aggressive phenotype. Cancer Res. 68, 1777-1785.

Lander, H. M., 1997. An essential role for free radicals and derived species in signal transduction. FASEB J. 11, 118-124.

Landis, J. R., Koch, G. G., 1977. The measurement of observer agreement for categorical data. Biometrics 33, 159-174.

Lardinois, O. M., Mestdagh, M. M., Rouxhet, P. G., 1996. Reversible inhibition and irreversible inactivation of catalase in presence of hydrogen peroxide. Biochim. Biophys. Acta 1295, 222-238.

Le Douarin, N. M., Ziller, C., Couly, G. F., 1993. Patterning of neural crest derivatives in the avian embryo: in vivo and in vitro studies. Dev. Biol. 159, 24-49.

Lefebvre, V., Behringer, R. R., de Crombrugghe, B., 2001. L-Sox5, Sox6 and Sox9 control essential steps of the chondrocyte differentiation pathway. Osteoarthr. Cartil. 9 (Suppl. A), S69-S75.

Lefebvre, V., Smits, P., 2005. Transcriptional control of chondrocyte fate and differentiation. Birth Defects Res. C. Embryo Today 75, 200-212.

Li, J., Stouffs, M., Serrander, L., Banfi, B., Bettiol, E., Charnay, Y., Steger, K., Krause, K. H., Jaconi, M. E., 2006. The NADPH oxidase NOX4 drives cardiac differentiation: role in regulating cardiac tran-scription factors and MAP kinase activation. Mol. Biol. Cell 17, 3978-3988.

Lieberman, D. E., McCarthy, R. C., 1999. The ontogeny of cranial base angulation in humans and chimpanzees and its implications for reconstructing pharyngeal dimensions. J. Hum. Evol. 36, 487-517.

Lieberman, D. E., Ross, C. F., Ravosa, M. J., 2000. The primate cranial base: Ontogeny, function, and integration. Am. J. Phys. Anthropol. 113, 117-169.

Little, C. B., Meeker, C. T., Hembry, R. M., Sims, N. A., Lawlor, K. E., Golub, S. B., Last, K., Fosang, A. J., 2005. Matrix metalloproteinases are not essential for aggrecan turnover during normal skeletal growth and development. Mol. Cell Biol. 25, 3388-3399.

Liu, Z., Xu, J., Colvin, J.S., Ornitz, D.M., 2002. Coordination of chondrogenesis and osteogenesis by fibroblast growth factor 18. Genes Dev. 16, 859-869.

Lu, J., Holmgren, A., 2009. Selenoproteins. J. Biol. Chem. 284, 723-727.

Mackie, E. J., Ahmed, Y. A., Tatarczuch, L., Chen, K. S., Mirams, M., 2008. Endochondral ossification: how cartilage is converted into bone in the developing skeleton. Int. J. Biochem. Cell Biol. 40, 46-62.

Mackie, E. J., Tatarczuch, L., Mirams, M., 2011. The skeleton: A multi-functional complex organ. The growth plate chondrocyte and endochondral ossification. J. Endocrinol. 211, 109-121.

Maeda, Y., Nakamura, E., Nguyen, M. T., Suva, L. J., Swain, F. L., Razzaque, M. S., Mackem, S., Lanske, B., 2007. Indian hedgehog produced by postnatal chondrocytes is essential for maintaining a growth plate and trabecular bone. PNAS 104, 6382-6387.

Mak, K. K., Kronenberg, H. M., Chuang, P. T., Mackem, S., Yang, Y., 2008. Indian hedgehog signals independently of PTHrP to promote chondrocyte hypertrophy. Develop. 135, 1947-1956.

Matos, L. L. D., Stabenow, E., Tavares, M. R., Ferraz, A. R., Capelozzi, V. L., Pinhal, M. A. D. S., 2006. Immunohistochemistry quantification by a digital computer-assisted method compared to semiquantitative analysis. Clinics (São Paulo) 61, 417-424.

Matsumoto, H., Silverton, S. F., Debolt, K., Shapiro, I. M., 1991. Superoxide dismutase and catalase activities in the growth cartilage: Relationship between oxidoreductase activity and chondrocyte maturation. J. Bone Min. Res. 6, 569-574.

Mills, G. C., 1957. Hemoglobin catabolism. I. Glutathione peroxidase, an erythrocyte enzyme which protects hemoglobin from oxidative breakdown. J. Biol. Chem. 229, 189-197.

Minina, E., Kreschel, C., Naski, M. C., Ornitz, D. M., Vortkamp, A., 2002. Interaction of FGF, Ihh/Pthlh, and BMP signaling integrates chondrocyte proliferation and hypertrophic differentiation. Dev. Cell 3, 439-449.

Minina, E., Wenzel, H. M., Kreschel, C., Karp, S., Gaffield, W., McMahon, A. P., Vortkamp, A., 2001. BMP and Ihh/PTHrP signaling interact to coordinate chondrocyte proliferation and differentiation. Develop. 128, 4523-4534.

Morita, K., Miyamoto, T., Fujita, N., Kubota, Y., Ito, K., Takubo, K., Miyamoto, K., Ninomiya, K., Suzuki, T., Iwasaki, R., Yagi, M., Takaishi, H., Toyama, Y., Suda, T., 2007. Reactive oxygen species induce chondrocyte hypertrophy in endochondral ossification. J. Exp. Med. 204, 1613-1623.

Mouakeh, M., 2001. Cephalometric evaluation of craniofacial pattern of Syrian children with Class III malocclusion. Am. J. Orthod. Dentofac. Orthop. 119, 640-649.

Muratori, M., Forti, G., Baldi, E., 2008. Comparing flow cytometry and fluorescence microscopy for analyzing human sperm DNA fragmentation by TUNEL labeling. Cytometry 73A, 785-787.

Nakamura, K., Shirai, T., Morishita, S., Uchida, S., Saeki-Miura, K., Makishima, F., 1999. p38 mitogen-activated protein kinase functionally contributes to chondrogenesis induced by growth/differentiation factor-5 in ATDC5 cells. Exp. Cell Res. 250, 351-363.

Netter, F. H., 2011. Atlas of human anatomy, Saunders/Elsevier, Philadelphia.

Ng, L. J., Wheatley, S., Muscat, G. E., Conway-Campbell, J., Bowles, J., Wright, E., Bell, D. M., Tam, P. P., Cheah, K. S., Koopman, P., 1997. SOX9 binds DNA, activates transcription, and coexpresses with type II collagen during chondrogenesis in the mouse. Dev. Biol. 183, 108-121.

Nilsson, O., Marino, R., De Luca, F., Phillip, M., Baron, J., 2005. Endocrine regulation of the growth plate. Horm. Res. 64, 157-165.

Niswander, L., 2003. Pattern formation: Old models out on a limb. Nat. Rev. Genet. 4, 133-143.

Noden, D. M., 1991. Cell movements and control of patterned tissue assembly during craniofacial development. J. Craniofac. Genet. Dev. Biol. 11, 192-213.

Olsen, B. R., Reginato, A. M., Wang, W., 2000. Bone development. Ann. Rev. Cell Dev. Biol. 16, 191-220.

Ong, C. W., Kim, L. G., Kong, H. H., Low, L. Y., Wang, T. T., Supriya, S., Kathiresan, M., Soong, R., Salto-Tellez, M., 2010. Computer-assisted pathological immunohistochemistry scoring is more time-effective than conventional scoring, but provides no analytical advantage. Histopathol. 56, 523-529.

Ornitz, D. M., 2005. FGF signaling in the developing endochondral skeleton. Cytokine Growth Fac. Rev. 16, 205-213.

Ortega, N., Behonick, D. J., Werb, Z., 2004. Matrix remodeling during endochondral ossification. Trends Cell Biol. 14, 86-93.

Otto, F., Thornell, A. P., Crompton, T., Denzel, A., Gilmour, K. C., Rosewell, I. R., Stamp, G. W., Beddington, R. S., Mundlos, S., Olsen, B. R., Selby, P. B., Owen, M. J., 1997. Cbfa1, a candidate gene for cleidocranial dysplasia syndrome, is essential for osteoblast differentiation and bone development. Cell 89, 765-771.

Pass, C., MacRae, V. E., Ahmed, S. F., Farquharson, C., 2009. Inflammatory cytokines and the GH/IGF-I axis: novel actions on bone growth. Cell Biochem. Funct. 27, 119-127.

Premkumar, S., 2011. Textbook of craniofacial growth, 1st ed., Jaypee Brothers Medical Publishers, New Delhi.

Proff, P., Will, F., Bokan, I., Fanghänel, J., Gedrange, T., 2008. Cranial base features in skeletal Class III patients. Angle Orthod. 78, 433-439.

Proffit, W. R., Fields, H. W., Sarver, D. M., 2007. Contemporary Orthodontics, Mosby Elsevier, St. Louis.

Pruszak, J., Sonntag, K.-C., Aung, M. H., Sanchez-Pernaute, R., Isacson, O., 2007. Markers and methods for cell sorting of human embryonic stem cell-derived neural cell populations. Stem Cells 25, 2257-2268.

Rahman, I., Biswas, S. K., 2006. OXIDANTS AND ANTIOXIDANTS / Antioxidants, Enzymatic. In: Laurent, G. J., Shapiro, S. D. (Ed.). Encyclopedia of Respiratory Medicine. Academic Press, Oxford, 258-266.

Rhee, S. G., 1999. Redox signaling: hydrogen peroxide as intracellular messenger. Exp. Mol. Med. 31, 53-59.

Rhee, S. G., Bae, Y. S., Lee, S. R., Kwon, J., 2000. Hydrogen peroxide: a key messenger that modulates protein phosphorylation through cysteine oxidation. Sci. STKE 2000, pe1.

Rocher, C., Lalanne, J. L., Chaudière, J., 1992. Purification and properties of a recombinant sulfur analog of murine selenium-glutathione peroxidase. Eur. J. Biochem. 205, 955-960.

Römer, P., Weingärtner, J., Roldán, J. C., Proff, P., Reicheneder, C., 2010. Development

dependent collagen gene expression in the rat cranial base growth plate. Ann. Anat. 192, 205-209.

Sablina, A. A., Budanov, A. V., Ilyinskaya, G. V., Agapova, L. S., Kravchenko, J. E., Chumakov, P. M., 2005. The antioxidant function of the p53 tumor suppressor. Nat. Med. 11, 1306-1313.

Sandell, L. J., Nalin, A. M., Reife, R. A., 1994. Alternative splice form of type II procollagen mRNA (IIA) is predominant in skeletal precursors and non-cartilaginous tissues during early mouse development. Dev. Dyn. 199, 129-140.

Sauer, H., Rahimi, G., Hescheler, J., Wartenberg, M., 2000. Role of reactive oxygen species and phosphatidylinositol 3-kinase in cardiomyocyte differentiation of embryonic stem cells. FEBS Lett. 476, 218-223.

Schmittgen, T. D., Livak, K. J., 2008. Analyzing real-time PCR data by the comparative C(T) method. Nat. Protoc. 3, 1101-1108.

Schultz, A. H., 1942. Conditions for balancing the head in primates. Am. J. Phys. Anthropol. 29, 483-497.

Scott, J. H., 1958. The cranial base. Am. J. Phys. Anthropol. 16, 319-348.

Shao, Y. Y., Wang, L., Ballock, R. T., 2006. Thyroid hormone and the growth plate. Rev. Endocr. Metab. Disord. 7, 265-271.

Shukunami, C., Ishizeki, K., Atsumi, T., Ohta, Y., Suzuki, F., Hiraki, Y., 1997. Cellular hypertrophy and calcification of embryonal carcinoma-derived chondrogenic cell line ATDC5 in vitro. J. Bone Min. Res. 12, 1174-1188.

Shukunami, C., Shigeno, C., Atsumi, T., Ishizeki, K., Suzuki, F., Hiraki, Y., 1996. Chondrogenic differentiation of clonal mouse embryonic cell line ATDC5 in vitro: Differentiation-dependent gene expression of parathyroid hormone (PTH)/PTH-related peptide receptor. J. Cell Biol. 133, 457-468.

Singh, G. D., McNamara, J. A., Lozanoff, S., 1997. Finite element analysis of the cranial base in subjects with Class III malocclusion. Br. J. Orthod. 24, 103-112.

Sperber, G. H., 1989. Craniofacial embryology, Wright, London.

Sperber, G. H., 2001. Craniofacial Development, B. C. Decker, Hamilton, Ont.

Stark, D., 1975. Embryologie, 3. Aufl. Thieme, Stuttgart.

Stevens, D. A., Hasserjian, R. P., Robson, H., Siebler, T., Shalet, S. M., Williams, G. R., 2000. Thyroid hormones regulate hypertrophic chondrocyte differentiation and expression of parathyroid hormone-related peptide and its receptor during endochondral bone formation. J. Bone Min. Res. 15, 2431-2442.

Stickens, D., Behonick, D. J., Ortega, N., Heyer, B., Hartenstein, B., Yu, Y., Fosang, A. J., Schorpp-Kistner, M., Angel, P., Werb, Z., 2004. Altered endochondral bone development in matrix metalloproteinase 13-deficient mice. Develop. 131, 5883-5895.

St-Jacques, B., Hammerschmidt, M., McMahon, A. P., 1999. Indian hedgehog signaling regulates proliferation and differentiation of chondrocytes and is essential for bone formation. Genes Dev. 13, 2072-2086.

Sun, J., Sun, Q., Lu, S., 2011. From selenoprotein to endochondral ossification: a novel mechanism with microRNAs potential in bone related diseases? Med. Hypotheses 77, 807-811.

Sundaresan, M., Yu, Z. X., Ferrans, V. J., Irani, K., Finkel, T., 1995. Requirement for generation of H_2O_2 for platelet-derived growth factor signal transduction. Science 270, 296-299.

Takahashi, T., Lord, B., Schulze, P. C., Fryer, R. M., Sarang, S. S., Gullans, S. R., Lee, R. T., 2003. Ascorbic acid enhances differentiation of embryonic stem cells into cardiac myocytes. Circulation 107, 1912-1916.

Taniguchi, N., Yoshida, K., Ito, T., Tsuda, M., Mishima, Y., Furumatsu, T., Ronfani, L., Abeyama, K., Kawahara, K., Komiya, S., Maruyama, I., Lotz, M., Bianchi, M. E., Asahara, H., 2007. Stage-specific secretion of HMGB1 in cartilage regulates endochondral ossification. Mol. Cell Biol. 27, 5650-5663.

Taylor, C. R., Levenson, R. M., 2006. Quantification of immunohistochemistry-issues concerning methods, utility and semiquantitative assessment II. Histopathol. 49, 411-424.

Temu, T. M., Wu, K. Y., Gruppuso, P. A., Phornphutkul, C., 2010. The mechanism of ascorbic acid-induced differentiation of ATDC5 chondrogenic cells. Am. J. Physiol. Endocrinol. Metab. 299, E325-E334.

Thomas, M., Jain, S., Kumar, G. P., Laloraya, M., 1997. A programmed oxyradical burst

causes hatching of mouse blastocysts. J. Cell Sci. 110 (Pt 14), 1597-1602.

Toppo, S., Flohé, L., Ursini, F., Vanin, S., Maiorino, M., 2009. Catalytic mechanisms and specificities of glutathione peroxidases: variations of a basic scheme. Biochim. Biophys. Acta 1790, 1486-1500.

Torous, D. K., Hall, N. E., Murante, F. G., Gleason, S. E., Tometsko, C. R., Dertinger, S. D., 2003. Comparative scoring of micronucleated reticulocytes in rat peripheral blood by flow cytometry and microscopy. Toxicol. Sci. 74, 309-314.

Tosatto, S. C., Bosello, V., Fogolari, F., Mauri, P., Roveri, A., Toppo, S., Flohé, L., Ursini, F., Maiorino, M., 2008. The catalytic site of glutathione peroxidases. Antioxid. Redox Signal. 10, 1515-1526.

Ursini, F., Maiorino, M., 2004. Glutathione Peroxidases. In: Lennarz, W. J., Lane, M. D. (Ed.). Encyclopedia of Biological Chemistry. Elsevier, New York, 224-228.

Ushio-Fukai, M., 2006. Redox signaling in angiogenesis: role of NADPH oxidase. Cardiovasc. Res. 71, 226-235.

Usui, M., Xing, L., Drissi, H., Zuscik, M., O'Keefe, R., Chen, D., Boyce, B. F., 2008. Murine and chicken chondrocytes regulate osteoclastogenesis by producing RANKL in response to BMP2. J. Bone Min. Res. 23, 314-325.

van der Earned, B. C., Karperien, M., Wit, J. M., 2003. Systemic and local regulation of the growth plate. Endocr. Rev. 24, 782-801.

van Engeland, M., Nieland, L. J., Ramaekers, F. C., Schutte, B., Reutelingsperger, C. P., 1998. Annexin V-affinity assay: a review on an apoptosis detection system based on phosphatidylserine exposure. Cytometry 31, 1-9.

Vogel, C., Marcotte, E. M., 2012. Insights into the regulation of protein abundance from proteomic and transcriptomic analyses. Nat. Rev. Genet. 13, 227-232.

Vortkamp, A., Lee, K., Lanske, B., Segre, G. V., Kronenberg, H. M., Tabin, C. J., 1996. Regulation of rate of cartilage differentiation by Indian hedgehog and PTH-related protein. Science 273, 613-622.

Wang, L., Shao, Y. Y., Ballock, R. T., 2007. Thyroid hormone interacts with the Wnt/beta–catenin signaling pathway in the terminal differentiation of growth plate chondrocytes. J.

Bone Min. Res. 22, 1988-1995.

Wang, L., Shao, Y. Y., Ballock, R. T., 2010. Thyroid hormone-mediated growth and differentiation of growth plate chondrocytes involves IGF-1 modulation of beta-catenin signaling. J. Bone Min. Res. 25, 1138-1146.

Weise, M., De-Levi, S., Barnes, K. M., Gafni, R. I., Abad, V., Baron, J., 2001. Effects of estrogen on growth plate senescence and epiphyseal fusion. PNAS 98, 6871-6876.

Williams, P. L., Bannister, L. H., Berry, M. M., Collins, P., Dyson, M., Dussek, J. E., Ferguson, M. W. J., 1995. Gray's anatomy, Churchill Livingstone, Edinburgh.

Wuelling, M., Vortkamp, A., 2010. Transcriptional networks controlling chondrocyte proliferation and differentiation during endochondral ossification. Pediatr. Nephrol. 25, 625-631.

Yadav, M. C., Simao, A. M., Narisawa, S., Huesa, C., McKee, M. D., Farquharson, C., Millan, J. L., 2011. Loss of skeletal mineralization by the simultaneous ablation of PHOSPHO1 and alkaline phosphatase function: a unified model of the mechanisms of initiation of skeletal calcification. J. Bone Min. Res. 26, 286-297.

Yao, Y., Wang, Y., 2013. ATDC5: An excellent in vitro model cell line for skeletal development. J. Cell Biochem. 114, 1223-1229.

Yoon, B. S., Lyons, K.M., 2004. Multiple functions of BMPs in chondrogenesis. J. Cell Biochem. 93, 93-103.

Yoon, B. S., Ovchinnikov, D. A., Yoshii, I., Mishina, Y., Behringer, R. R., Lyons, K. M., 2005. Bmpr1a and Bmpr1b have overlapping functions and are essential for chondrogenesis in vivo. Proc. Natl. Acad. Sci. USA 102, 5062-5067.

Yoon, B. S., Pogue, R., Ovchinnikov, D. A., Yoshii, I., Mishina, Y., Behringer, R. R., Lyons, K. M., 2006. BMPs regulate multiple aspects of growth-plate chondrogenesis through opposing actions on FGF pathways. Develop. 133, 4667-4678.

Zhang, G., Gurtu, V., Kain, S. R., Yan, G., 1997. Early detection of apoptosis using a fluorescent conjugate of annexin V. Biotechniques 23, 525-531.

List of figures

List of tables

List of abbreviations

°C	Degree Celsius; temperature
AA	Antibiotics and antimycotics
ALP	Alkaline phosphatase
APS	Ammonium persulfate
Asn	Asparagine amino acid
BMP2	Bone morphogenetic protein-2
BMPs	Bone morphogenetic proteins
cDNA	Complementary DNA
CO_2	Carbon dioxide
Col10a1	Collagen, type X, alpha 1
Col2a1	Collagen, type II, alpha 1
DNA	Deoxyribonucleic acid
EDTA	Ethylenediaminetetraacetic acid
ERKs	Extracellular-signal-regulated kinases
FCS	Fetal calf serum
FGFR3	Fibroblast growth factor receptor-3
FGFs	Fibroblast growth factors
FITC	Fluorescein isothiocyanate
g	Gram; mass
GH	Growth hormone / somatotropin
Gli	Gli family of transcription factors
Gln	Glutamine amino acid

Gpx1	Glutathione peroxidase-1
Gpx2	Glutathione peroxidase-2 (gastrointestinal)
Gpx3	Glutathione peroxidase-3 (plasma)
Gpx4	Glutathione peroxidase-4 (phospholipid hydroperoxidase)
Gpx5	Glutathione peroxidase-5 (epididymal androgen-related protein)
Gpxs	Glutathione peroxidases
GSH	Glutathione
GSSG	Glutathione disulfide
h	Hour; time
H_2O	Water
H_2O_2	Hydrogen peroxide
HCl	Hydrogen chloride
HMGB1	High-mobility group protein B1
Hox	Homeodomain
IGF1	Insulin-like growth factor-1
Ihh	Indian hedgehog
JNKs	c-Jun N-terminal kinases
LacZ	β-galactosidase
LB medium	Lysogeny broth medium
LDH	Lactate dehydrogenase
M	Molar; concentration
mA	Milliampere; electric current
mg/ml	Milligrams per millilitre; density

min	Minute; time
ml	Millilitre; volume
mM	Millimolar; concentration
M-MLV	Moloney murine leukemia virus
MMP13	Matrix metalloproteinase-13
MMP9	Matrix metalloproteinase-9
MMPs	Matrix metalloproteinases
mRNA	Messenger RNA
NaCl	Sodium chloride
N-CAM	Neural cell adhesion molecule
ng/µl	Nanograms per microlitre; density
nM	Nanomolar; concentration
nm	Nanometre; wavelength
Nox4/1/2	Genes encoding NADPH oxidases
p38	p38 mitogen-activated protein kinases
PGF2a	Prostaglandin-F2a
PGG2	Prostaglandin-G2
pH	Measure of acidity or alkalinity
PHOSPHO1	Phosphatase, orphan-1
PI	Propidium iodide
pmol/µl	Picomoles per microlitre
Polr2a	Polymerase (RNA) II (DNA directed) polypeptide A
PTHrP	Parathyroid hormone-related protein

PTHrP-R	Receptor of parathyroid hormone-related protein
PVDF	Polyvinylidene fluoride
qRT-PCR	Real time quantitative reverse transcription polymerase chain reaction
RANKL	Receptor activator of nuclear factor kappa-B ligand
RNA	Ribonucleic acid
ROOH	Alkyl hydroperoxides
ROS	Reactive oxygen species
rpm	Revolutions per minute; frequency of rotation
Runx2	Runt-related transcription factor-2
SDS	Sodium dodecyl sulfate
Se	Selenium
Sec	Selenocysteine
sec	Second; time
Shh	Sonic hedgehog
SOD	Superoxide dismutases
Sox9	Transcription factor Sox9
T_3	Triiodothyronine
Tak1	Transforming growth factor-β activated kinase-1
TBS-T	Tris-buffered saline additionally containing Tween 20
TEMED	Tetramethylethylenediamine
TGF-β	Transforming growth factor-β
TNAP	Tissue-nonspecific alkaline phosphatase
Tris	Tris(hydroxymethyl)aminomethane

Trp	Tryptophan amino acid
V	Volt; voltage
VEGFs	Vascular endothelial growth factors
Wnt	Wnt signalling pathway
µg	Microgram; mass
µg/ml	Micrograms per millilitre; density
µl	Microlitre; volume
µm	Micrometre; length
µM	Micromolar; concentration

Declaration of academic honesty / Eidesstattliche Erklärung

I herewith declare that the submitted dissertation has been composed by myself without any inadmissible help and without the use of sources other than those given due reference in the text and listed in the list of references. I further declare that all persons and institutions that have directly or indirectly helped me with the preparation of the dissertation have been acknowledged and that this dissertation has not been submitted, wholly or substantially, as an examination document at any other institution.

Freiberg, 09.01.2016

Vasiliki Koretsi

Hiermit erkläre ich, dass ich die hier vorliegende Dissertation selbstständig verfasst und keine anderen als die angegebenen Hilfsmittel benutzt habe. Die Dissertation ist bisher keiner anderen Fakultät vorgelegt worden. Ich erkläre, dass ich bisher kein Promotionsverfahren erfolglos beendet habe und dass eine Aberkennung eines bereits erworbenen Doktorgrades nicht vorliegt.

Freiberg, 09.01.2016

Vasiliki Koretsi

Acknowledgements

I am very thankful to the director of the department, Professor Dr. Dr. Peter Proff, for offering me the opportunity to conduct research at his department.

In addition, I would like to thank Priv. - Doz. Dr. Piero Römer for his scientific guidance, which made this work possible.

A very special thanks to Professor Dr. Jochen Fanghänel for revising the manuscript and providing vital advice.

I also wish to express my sincere gratitude to Mrs. Kathrin Bauer, who was generously helpful and offered me valuable assistance, support, and guidance.

I thank Dr. Christian Kirschneck for providing statistical advice.

Last but not least, I would like to thank the members of my family for their invaluable support and encouragement in every step of my life, without which I could not have been able to fulfil my dreams.

Freiberg, 09.01.2016

Vasiliki Koretsi